



HAL
open science

Correlated Evolution of two Copulatory Organs via a Single Cis-Regulatory Nucleotide Change

Olga Nagy, Isabelle Nuez, Rosina Savisaar, Alexandre E. Peluffo, Amir Yassin, Michael Lang, David L Stern, Daniel R Matute, Jean R David, Virginie Courtier-Orgogozo

► **To cite this version:**

Olga Nagy, Isabelle Nuez, Rosina Savisaar, Alexandre E. Peluffo, Amir Yassin, et al.. Correlated Evolution of two Copulatory Organs via a Single Cis-Regulatory Nucleotide Change. *Current Biology - CB*, 2018, 28 (21), pp.3450-3457. 10.1016/j.cub.2018.08.047 . hal-01887693

HAL Id: hal-01887693

<https://hal.science/hal-01887693>

Submitted on 4 Oct 2018

HAL is a multi-disciplinary open access archive for the deposit and dissemination of scientific research documents, whether they are published or not. The documents may come from teaching and research institutions in France or abroad, or from public or private research centers.

L'archive ouverte pluridisciplinaire **HAL**, est destinée au dépôt et à la diffusion de documents scientifiques de niveau recherche, publiés ou non, émanant des établissements d'enseignement et de recherche français ou étrangers, des laboratoires publics ou privés.



Distributed under a Creative Commons Attribution - NonCommercial - NoDerivatives 4.0 International License

1 **Correlated Evolution of two Copulatory Organs via a Single Cis-Regulatory Nucleotide**
2 **Change**

3 Olga Nagy¹, Isabelle Nuez¹, Rosina Savisaar^{1†}, Alexandre E. Peluffo¹, Amir Yassin², Michael Lang¹,
4 David L. Stern³, Daniel R. Matute⁴, Jean R. David^{2,5} and Virginie Courtier-Orgogozo^{1,6,*}

5
6 ¹Institut Jacques Monod, CNRS UMR7592, Univ. Paris-Diderot, 75013 Paris, France.

7 ²Institut Systématique Évolution Biodiversité (ISYEB), Centre National de Recherche Scientifique,
8 MNHN, Sorbonne Université, EPHE, 57 rue Cuvier, CP 50, 75005 Paris, France

9 ³Janelia Research Campus, 19700 Helix Drive, Ashburn, Virginia 20147.

10 ⁴Biology Department, University of North Carolina, Chapel Hill, USA.

11 ⁵Laboratoire Evolution, Génomes, Comportement, Biodiversité (EGCE), CNRS, IRD, Univ. Paris-
12 sud, Univ. Paris-Saclay, 91198 Gif-sur-Yvette, France.

13 ⁶Lead Contact

14 *Correspondence: virginie.courtier@normalesup.org, @Biol4Ever, +33 1 57 27 80 43

15 †current address: The Milner Centre for Evolution, Department of Biology and Biochemistry,
16 University of Bath, Bath BA2 7AY, UK.

17

18 **One Sentence Summary:** We identify one nucleotide substitution in a gene regulatory region
19 contributing to evolutionary change of two distinct copulatory organs.

20

21 **Highlights:**

- 22 - We identify a gene and 3 substitutions causing genital evolution between species
- 23 - The evolved mutations lie in a pleiotropic enhancer
- 24 - One mutation decreases genital bristle number and increases leg sex comb tooth number
- 25 - This mutation disrupts a binding site for Abd-B in genitals and for another factor in legs

26

27 **SUMMARY**

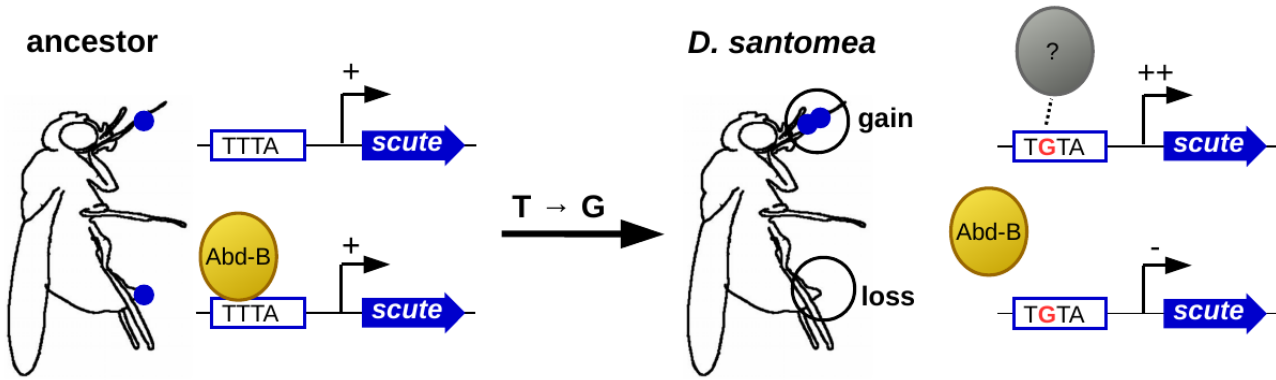
28 **Diverse traits often covary between species [1–3]. The possibility that a single mutation could**
29 **contribute to the evolution of several characters between species [3] is rarely investigated as**
30 **relatively few cases are dissected at the nucleotide level. *Drosophila santomea* has evolved**
31 **additional sex comb sensory teeth on its legs and has lost two sensory bristles on its genitalia.**
32 **We present evidence that a single nucleotide substitution in an enhancer of the *scute* gene**
33 **contributes to both changes. The mutation alters a binding site for the Hox protein**
34 **Abdominal-B in the developing genitalia, leading to bristle loss, and for another factor in the**
35 **developing leg, leading to bristle gain. Our study suggests that morphological evolution**
36 **between species can occur through a single nucleotide change affecting several sexually**
37 **dimorphic traits.**

38 (126 words)

39

40 **Keywords:** pleiotropy, cis-regulatory, sensory organ, *Drosophila*, copulation, genitalia,
41 hypandrium, sex comb, microevolution, *scute*, *Abd-B*

42 **Graphical Abstract:**



43

44

45 **RESULTS AND DISCUSSION**

46 “Variability is governed by many unknown laws, of which correlated growth is probably the most
47 important.” [1]

48 Correlated evolution of traits is widespread among taxa [1,2] and can be due to pleiotropy, where a
49 single locus causally affects several traits [3]. Pleiotropy imposes large constraints on the paths of
50 evolution [4,5], making it crucial to assess the extent of pleiotropy to understand the evolutionary
51 process. Empirical studies suggest that many loci influence multiple traits [3,6,7] and current data
52 cannot reject the idea that all genetic elements have pleiotropic roles [3,8,9]. Several pleiotropic
53 substitutions have been associated with natural variation [10–13]: most are coding changes and all
54 underlie intraspecific changes (www.gephebase.org). Nevertheless it remains unclear whether
55 pleiotropic mutations contribute also to interspecific evolution, as experimental evidence suggests
56 that the mutations responsible for interspecies evolution may be less pleiotropic than the mutations
57 underlying intraspecific variation [14].

58 Here we focused on male sexual bristle evolution between *Drosophila yakuba* and
59 *Drosophila santomea*, which diverged approximately 0.5-1 million years ago [15] and can produce
60 fertile F1 females in the laboratory [16], facilitating genetic mapping. We found that hypandrial
61 bristles – two prominent mechanosensory bristles located on the ventral part of male genitalia in all
62 *D. melanogaster* subgroup species – are missing in *D. santomea* males (Figure 1). Examination of
63 many inbred stocks and 10 closely related species revealed that the absence of hypandrial bristles is
64 a derived *D. santomea*-specific trait (Figure 1, see also Extra Tables). No other genital bristle type
65 was noticeably variable in number between *D. yakuba* and *D. santomea* (see Extra Figures).

66 We performed whole-genome QTL mapping between *D. santomea* and *D. yakuba* and found
67 that the left tip of chromosome X explains 44% of the variance in hypandrial bristle number in each
68 backcross (confidence interval = 7 Mb for the *D. santomea* backcross and 2.6 Mb for the *D. yakuba*
69 backcross, Figure 2A). Duplication mapping in rare *D. santomea*-*D. melanogaster* hybrid males
70 narrowed down the causal region to a 84.6 kb region of the *achaete-scute* complex (AS-C) (Figure
71 2B-C, see also Extra Tables).

72 The AS-C locus contains four genes, but only two, *achaete* (*ac*) and *scute* (*sc*), are required
73 for bristle formation [17]. Both genes are co-expressed, share *cis*-regulatory elements and act
74 redundantly to specify bristles [18,19]. The elaborate expression pattern of *ac* and *sc* genes
75 prefigures the adult bristle pattern and is controlled by numerous *cis*-regulatory elements [18]. We
76 tested which of the two genes, *ac* or *sc*, contributes to loss of bristles using null mutants in *D.*
77 *melanogaster*. All *ac*^{CAMI} null mutant males had 2 hypandrial bristles (n=15) and *sc*^{M6} null mutants
78 had none (n=15) (Tables S1-2), indicating that *sc* is required for hypandrial bristle development in
79 *D. melanogaster*.

80 We detected 64 nucleotide differences in the *sc* coding region between *D. yakuba* and *D.*

81 *santomea*, and all were synonymous substitutions, indicating that coding changes in *sc* are not
82 responsible for the evolved function of *sc*. Using molecularly mapped chromosomal aberrations, we
83 identified a 5-kb region located > 46 kb downstream of the *sc* promoter that is required in *D.*
84 *melanogaster* for hypandrial bristle development (Figure S1A, see also Extra Figures, Tables S1-2).
85 Independently we screened 55 *GAL4* reporter constructs tiling the entire *AS-C* locus and identified
86 three *GAL4* lines (*15E09*, *054839* and *18C05*) that drive expression in hypandrial bristles (Figures
87 2C and S1B-E, see also Extra Tables). Only one of these lines, *18C05*, increased hypandrial bristle
88 number with *UAS-scute* in a *sc* mutant background or in a *sc*⁺ background (Figures 2C and S1F-Q,
89 see also Extra Figures). The 2036-bp *18C05* region is located within the 5-kb candidate region
90 identified with *ac-sc* structural mutations (Figure 2C), suggesting that *18C05* is a good candidate
91 region for hypandrial bristle evolution.

92 To test whether loss of hypandrial bristles in *D. santomea* resulted from changes(s) in the
93 *18C05 cis*-regulatory region, we assayed whether orthologous *18C05* regions from *D.*
94 *melanogaster*, *D. yakuba* and *D. santomea* driving a *sc* coding region could rescue hypandrial
95 bristles in a *D. melanogaster sc* mutant. The *D. melanogaster 18C05* enhancer rescued two bristles
96 in both *sc*²⁹ and *sc*^{M6} mutant backgrounds, indicating that this construct mimics normal levels of *sc*
97 expression (Figure 3). The *D. yakuba 18C05* enhancer rescued on average 2 hypandrial bristles in
98 *sc*^{M6} and 0.5 bristles in *sc*²⁹ whereas the *D. santomea 18C05* enhancer rescued significantly fewer
99 bristles (1.1 in *sc*^{M6} and 0 bristles in *sc*²⁹, Figure 3). For another measure of *18C05* enhancer activity,
100 we compared the ability of enhancer-*GAL4* constructs containing the *18C05* region from *D.*
101 *melanogaster*, *D. yakuba* or *D. santomea* to induce extra bristles in *sc* mutants using the *UAS-GAL4*
102 system with *UAS-sc*. In this assay the *D. santomea 18C05* region also induced fewer bristles than
103 the corresponding *D. yakuba* region (Figure 3, GLM-Quasi-Poisson, $F(19, 509) = 161.7$, $p < 10^{-5}$
104 for *sc*²⁹; $F(19, 415) = 125.9$, $p < 10^{-5}$ for *sc*^{M6}). Together, these results suggest that changes(s) within
105 *18C05* contributed to hypandrial bristle evolution in *D. santomea*.

106 To narrow down the region responsible for hypandrial bristle loss, we dissected the *18C05*
107 element from *D. melanogaster*, *D. yakuba* and *D. santomea* into smaller overlapping pieces and
108 quantified their ability to produce hypandrial bristles with the *GAL4* rescue experiment. For all
109 three species we found that smaller segments rescued significantly fewer bristles than the
110 corresponding full region (Figure S2A-B, see also Extra Figures). Thus, transcription factor binding
111 sites scattered throughout the entire ~2 kb of the *18C05* element are required to drive full
112 expression in the hypandrial bristle region.

113 Sequence alignment of the *18C05* region from multiple species revealed 11 substitutions and
114 one indel that are fixed and uniquely derived in *D. santomea*. Among them, seven substitutions
115 altered sites that are otherwise conserved in the *D. melanogaster* subgroup (Extra Figures). We
116 tested the effect of these seven *D. santomea*-specific nucleotide changes by introducing them one at
117 a time or all together, into either a *D. yakuba 18C05* enhancer or into the inferred ancestral enhancer
118 driving *sc* expression (Figure S2, see also Extra Tables and Extra Figures). The ancestral *18C05*
119 sequence was resurrected by reverting the *D. santomea*-specific and *D. yakuba*-specific mutations
120 to their ancestral states and it produced the same number of bristles as the *D. yakuba* construct
121 (Figure 3, Extra Figures). Four substitutions (*G869A*, *T970A*, *T1008C* and *T1482C*) had no effect,
122 whether in the *D. yakuba* or in the ancestral background (GLM-Quasi-Poisson, $p > 0.6$). Three
123 substitutions (*T1429G*, *A1507G* and *T1775G*) decreased the number of rescued bristles in both the
124 *D. yakuba* and the ancestral sequence, and these effects were highly significant, except for *A1507G*
125 in the *D. yakuba* background, which was slightly above statistical threshold (using the most
126 stringent correction method) (Figure 3). These results are consistent with analysis of smaller pieces
127 of *18C05* and of *18C05* chimeric constructs containing DNA fragments from *D. yakuba* and *D.*
128 *santomea* (Figure S2C). When combined into the *D. yakuba* background, the seven *D. santomea*-
129 specific substitutions rescued the same number of bristles as the *D. santomea 18C05* construct
130 (Figure 3, GLM-Quasi-Poisson, $p > 0.9$ in *sc*^{M6}). We conclude that at least three fixed substitutions

130 within a 350-bp region located 49 kb away from *sc* contribute to the reduction in hypandrial bristle
131 number in *D. santomea*.

132 Analysis of *18C05-GAL4* and *18C05-GFP* reporter constructs revealed that the *18C05*
133 region drives expression not only in male genital discs [20] but also in male developing forelegs in
134 the presumptive sex comb domain [21](Figure 4A-B,D-F). The *18C05-GFP* reporter constructs
135 drive expression in fewer cells than *sc-GFP* (Fig. 4C), indicating that *sc* expression in the
136 presumptive sex comb domain is also regulated by cis-regulatory regions outside of *18C05*. Sex
137 combs are sensory organs used for grasping the female during copulation [22]. They differ in bristle
138 number between *D. santomea* and *D. yakuba* (Figure 4G-I, see also Extra Figures), and 35% of the
139 species difference is attributed to the X chromosome [23], where *sc* is located. These results
140 prompted us to test whether the mutations contributing to hypandrial bristle evolution also affect
141 sex combs. Significantly more GFP-positive cells were detected in the first tarsal segment at 5h
142 after puparium formation (APF) with *18C05yakT1775G-GFP* than with *18C05yak-GFP* (GLM-
143 Poisson, Chi-squared (20,2) deviance = 9.75, $p = 0.033$), suggesting that *T1775G* increases *sc*
144 expression in the first tarsal segment. Sex comb tooth number was reduced in *sc^{M6}* and *sc⁶*
145 and significantly rescued with several *18C05-sc* constructs (Figure 4J-K). Analysis of *sc^{M6}* and *sc⁶*
146 mutants rescued with the *yak18C05-sc* constructs containing the *D. santomea*-specific substitutions
147 showed that *T1429G* and *T1507G* have no effect and that *T1775G* increases the number of sex
148 comb teeth (Figure 4J-K). We conclude that the *T1775G* substitution contributes to both the
149 increase in sex comb tooth number and the loss of hypandrial bristles.

150 A bioinformatics search revealed that the *T1775G* substitution is predicted to alter a binding
151 site for the Hox protein Abdominal-B (*Abd-B*) (Table S3). *Abd-B* is expressed only in the posterior
152 part of the fly, where it directs the development of posterior-specific structures such as the genitalia
153 [24]. We found that reducing *Abd-B* expression, using either genetic mutations or RNA interference,
154 resulted in loss of hypandrial bristles (Figure S3 and Table S4), indicating that normal levels of
155 *Abd-B* expression are required for hypandrial bristle development. Electrophoretic mobility shift
156 assays showed that *Abd-B* proteins bind more strongly to a 54-bp fragment of the *18C05* sequence
157 containing the *D. yakuba*-specific T at position 1775 than the *D. santomea*-specific G at this
158 position (Figure S4). These results are consistent with the hypothesis that the *T1775G* substitution
159 decreases *ABD-B* binding, contributing to reduction in *sc* expression levels, and ultimately reducing
160 the number of hypandrial bristles. Since *Abd-B* is not expressed in developing legs, *T1775G* is
161 expected to affect binding of other factors to increase sex comb tooth number. Overall, our study
162 suggests that *T1775G* alters overlapping binding sites for distinct factors in the leg and the genitalia.
163 All our analyses of the effects of individual substitutions have been carried out in *D. melanogaster*
164 background. It is thus possible that the *18C05* enhancer represents only part of the effect of the *sc*
165 locus on bristle divergence.

166 Intriguingly, the two organs affected by substitution *T1775G* – hypandrial bristles and sex
167 combs – may both aid the male to position himself on top of the female during copulation [22,25].
168 Genitals are the most rapidly evolving organs in animals with internal fertilization [26]. To our
169 knowledge, only two other mutations contributing to the evolution of genital anatomy are known.
170 First, a 61-kb-deletion of a cis-regulatory region of the *androgen receptor (AR)* gene in humans is
171 associated with loss of keratinized penile spines in humans compared to chimpanzees [27]. Second,
172 an amino acid change in the *nath10 acetyltransferase* gene which probably appeared recently in
173 laboratory strains of the nematode *C. elegans*, alters morphology in the presence of some mutations
174 but not in a wild-type genetic background [10]. Both mutations appear to be pleiotropic: the *AR*
175 deletion is associated with loss of facial vibrissae in humans and the *nath10* mutation affects egg
176 and sperm production as well. The paucity of known mutations responsible for genital evolution
177 makes it currently difficult to propose general rules for the causes of rapid genital evolution. Our
178 results are reminiscent of Mayr's pleiotropy hypothesis [28], which posits that certain characters
179 may evolve arbitrarily as a result of selection on other traits due to pleiotropic mutations. In our

180 case, whether the evolutionary change in sex comb tooth number or in genital bristle number has
181 any effect on fitness is unknown.

182 We report here the first experimental evidence for a cis-regulatory substitution between
183 species with pleiotropic effects. Given the large number of bristle types regulated by *sc* (>100 in
184 adult flies), it is possible that no cis-regulatory mutation in *sc* can affect only one bristle type. Our
185 results challenge the idea that cis-regulatory enhancers are strict tissue-specific modules underlying
186 evolutionary changes in targeted traits [29]. Even though cis-regulatory mutations may affect
187 several tissues, it is probable that they still tend to be less pleiotropic than coding changes. Our
188 results are thus compatible with the idea that cis-regulatory changes tend to have fewer pleiotropic
189 effects than coding changes on average. Enhancer sequences evolve rapidly, with rapid turn over of
190 individual binding sites while maintaining transcriptional output over millions of years by
191 compensatory mutations [30]. Since pleiotropic mutations can have deleterious off-target effects,
192 we propose that evolution of pleiotropic sites within enhancers should trigger the subsequent
193 selection of compensatory mutations in cis, thus contributing to rapid divergence of cis-regulatory
194 sequences. Overall, our results suggest that pleiotropic cis-regulatory mutations may play a more
195 important role in evolution than previously thought.

196

197 ACKNOWLEDGEMENTS

198 We thank the Tucson Drosophila Species Stock Center, the VDRC, Kyoto and Bloomington Stock
199 Centers for flies. We thank São Tomé authorities for allowing us to collect flies. We thank S. Picard
200 for help with MSG, E. Sánchez-Herrero for *Abd-B* flies, F. Schweisguth for *GFP-sc* flies, J. Selegue
201 and S.B. Carroll for the *Abd-B* construct, L. Pintard and N. Joly for help in protein purification, R.
202 Mann, S. Feng and G. Rice for EMSA and immunostaining suggestions, F. Mallard and T. Tully for
203 advices on the statistical analyses, J. L. Villanueva-Cañas for help with JASPAR. We thank Q.D.
204 Tran, M. Notin, V. Ludger, A. Matamoro-Vidal, C. Nobre, G. Verebes, S. El Ouisi, A. La, F. Foutel-
205 Rodier, C. Guillard-Sirieix and A. Aydogan for their contributions and C. Desplan, D. Petrov, B.
206 Prud'homme, A. Martin and J.A. Lepesant for comments on the manuscript. We acknowledge the
207 ImagoSeine core facility of the Institut Jacques Monod, member of IBiSA and France-BioImaging
208 (ANR-10-INBS-04) infrastructures. We thank the Courtier-Orgogozo team for providing a
209 stimulating environment and technical support.

210

211 FUNDING

212 The research leading to this paper has received funding from the European Research Council under
213 the European Community's Seventh Framework Program (FP7/2007-2013 Grant Agreement no.
214 337579) to VCO, from the labex "Who am I?" (ANR-11-LABX-0071) funded by the French
215 government through grant no. ANR-11-IDEX-0005-02 to AEP and from NIH (1R01GM121750) to
216 DRM.

217

218 AUTHOR CONTRIBUTIONS

219 J.R.D. found that *D. santomea* lacks hypandrial bristles and that the trait difference is X-linked,
220 D.L.S. genotyped flies with MSG, A.Y., I.N. and V.C.O. performed the QTL mapping experiment,
221 D.R.M. made the *D. santomea-D. melanogaster* hybrids, I.N. dissected them, O.N. did all other fly
222 crosses and dissected them, O.N., I.N., R.S. and A.E.P. phenotyped >3000 males for hypandrial
223 bristles, O.N. phenotyped all other bristles, O.N. and M.L. did EMSA, O.N. and I.N. constructed
224 the plasmids, O.N. performed immunostainings and microscopy, A.E.P. performed all statistical
225 analyses with feedback from O.N. and M.L., D.R.M. collected wild flies, V.C.O. supervised

226 research, performed bioinformatics sequence analysis and wrote the paper with O.N. All authors
227 provided feedback on the text.

228

229 **DECLARATION OF INTEREST**

230 The authors declare no competing interests.

231

232 **REFERENCES**

- 233 1. Darwin, C. (1859). On the origin of species by means of natural selection, or the preservation
234 of favoured races in the struggle for life (John Murray).
- 235 2. Saltz, J.B., Hessel, F.C., and Kelly, M.W. (2017). Trait Correlations in the Genomics Era.
236 *Trends Ecol. Evol.* 32, 279–290.
- 237 3. Paaby, A.B., and Rockman, M. V. (2013). The many faces of pleiotropy. *Trends Genet.* 29,
238 66–73.
- 239 4. Fisher, R.A. (1930). *The genetical theory of natural selection* (Oxford: Clarendon).
- 240 5. Orr, H.A. (2000). Adaptation and the cost of complexity. *Evolution* (N. Y). 54, 13–20.
- 241 6. Wagner, G.P., and Zhang, J. (2011). The pleiotropic structure of the genotype–phenotype
242 map: the evolvability of complex organisms. *Nat. Rev. Genet.* 12, 204–213.
- 243 7. Stearns, F.W. (2010). One Hundred Years of Pleiotropy: A Retrospective. *Genetics* 186, 767–
244 773.
- 245 8. Lonfat, N., Montavon, T., Darbellay, F., Gitto, S., and Duboule, D. (2014). Convergent
246 evolution of complex regulatory landscapes and pleiotropy at Hox loci. *Science* (80-.). 346,
247 1004–1006.
- 248 9. Preger-Ben Noon, E., Sabarís, G., Ortiz, D.M., Sager, J., Liebowitz, A., Stern, D.L., and
249 Frankel, N. (2018). Comprehensive Analysis of a cis -Regulatory Region Reveals Pleiotropy
250 in Enhancer Function. *Cell Rep.* 22, 3021–3031.
- 251 10. Duvéau, F., and Félix, M.-A. (2012). Role of pleiotropy in the evolution of a cryptic
252 developmental variation in *Caenorhabditis elegans*. *PLoS Biol.* 10, e1001230.
- 253 11. Chang, S.H., Jobling, S., Brennan, K., and Headon, D.J. (2009). Enhanced Edar Signalling
254 Has Pleiotropic Effects on Craniofacial and Cutaneous Glands. *PLoS One* 4, e7591.
- 255 12. Kent, C.F., Daskalchuk, T., Cook, L., Sokolowski, M.B., and Greenspan, R.J. (2009). The
256 *Drosophila* foraging Gene Mediates Adult Plasticity and Gene–Environment Interactions in
257 Behaviour, Metabolites, and Gene Expression in Response to Food Deprivation. *PLOS*
258 *Genet.* 5, e1000609.

- 259 13. Endler, L., Gibert, J.M., Nolte, V., and Schlötterer, C. (2018). Pleiotropic effects of regulatory
260 variation in tan result in correlation of two pigmentation traits in *Drosophila melanogaster*.
261 *Mol. Ecol.* 27(16), 3207-3218.
- 262 14. Stern, D.L., and Orgogozo, V. (2008). The loci of evolution: How predictable is genetic
263 evolution? *Evolution* 62, 2155–2177.
- 264 15. Turissini, D.A., and Matute, D.R. (2017). Fine scale mapping of genomic introgressions
265 within the *Drosophila yakuba* clade. *PLoS Genet.* 13, e1006971.
- 266 16. Lachaise, D., Harry, M., Solignac, M., Lemeunier, F., Bénassi, V., and Cariou, M.L. (2000).
267 Evolutionary novelties in islands: *Drosophila santomea*, a new melanogaster sister species
268 from São Tomé. *Proceedings. Biol. Sci.* 267, 1487–1495.
- 269 17. Simpson, P., Woehl, R., and Usui, K. (1999). The development and evolution of bristle
270 patterns in Diptera. *Development* 126, 1349–1364.
- 271 18. Gómez-Skarmeta, J.L., Rodríguez, I., Martínez, C., Culi, J., Ferrés-Marcó, D., Beamonte, D.,
272 and Modolell, J. (1995). Cis-regulation of achaete and scute: shared enhancer-like elements
273 drive their coexpression in proneural clusters of the imaginal discs. *Genes Dev.* 9, 1869–
274 1882.
- 275 19. Marcellini, S., Gibert, J.-M., and Simpson, P. (2005). achaete, but not scute, is dispensable
276 for the peripheral nervous system of *Drosophila*. *Dev. Biol.* 285, 545–553.
- 277 20. Jory, A., Estella, C., Giorgianni, M.W., Slattery, M., Lavery, T.R., Rubin, G.M., and Mann,
278 R.S. (2012). A Survey of 6,300 Genomic Fragments for cis-Regulatory Activity in the
279 Imaginal Discs of *Drosophila melanogaster*. *Cell Rep.* 2, 1014–1024.
- 280 21. Tanaka, K., Barmina, O., Sanders, L.E., Arbeitman, M.N., and Kopp, A. (2011). Evolution of
281 sex-specific traits through changes in HOX-dependent doublesex expression. *PLoS Biol.* 9,
282 e1001131.
- 283 22. Ng, C.S., and Kopp, A. (2008). Sex combs are important for male mating success in
284 *Drosophila melanogaster*. *Behav. Genet.* 38, 195.
- 285 23. Coyne, J.A., Elwyn, S., Kim, S.Y., and Llopart, A. (2004). Genetic studies of two sister
286 species in the *Drosophila melanogaster* subgroup, *D. yakuba* and *D. santomea*. *Genet. Res.*
287 (Camb). 84, 11–26.
- 288 24. Foronda, D., Estrada, B., de Navas, L., and Sánchez-Herrero, E. (2006). Requirement of
289 Abdominal-A and Abdominal-B in the developing genitalia of *Drosophila* breaks the
290 posterior downregulation rule. *Development* 133, 117–127.
- 291 25. Hurtado-Gonzales, J.L., Gallaher, W., Warner, A., and Polak, M. (2015). Microscale Laser
292 Surgery Demonstrates the Grasping Function of the Male Sex Combs in *Drosophila*
293 *melanogaster* and *Drosophila bipectinata*. *Ethology* 121, 45–56.
- 294 26. Eberhard, W.G. (1988). *Sexual Selection and Animal Genitalia* (Harvard University Press).

- 295 27. McLean, C.Y., Reno, P.L., Pollen, A.A., Bassan, A.I., Capellini, T.D., Guenther, C., Indjeian,
296 V.B., Lim, X., Menke, D.B., Schaar, B.T., *et al.* (2011). Human-specific loss of regulatory
297 DNA and the evolution of human-specific traits. *Nature* 471, 216–219.
- 298 28. Mayr, E. (1963). *Animal species and evolution* (Harvard University Press).
- 299 29. Carroll, S.B. (2008). Evo-devo and an expanding evolutionary synthesis: a genetic theory of
300 morphological evolution. *Cell* 134, 25–36.
- 301 30. Cheng, Y., Ma, Z., Kim, B.-H., Wu, W., Cayting, P., Boyle, A.P., Sundaram, V., Xing, X.,
302 Dogan, N., Li, J., *et al.* (2014). Principles of regulatory information conservation between
303 mouse and human. *Nature* 515, 371.
- 304 31. Andolfatto, P., Davison, D., Erezyilmaz, D., Hu, T.T., Mast, J., Sunayama-Morita, T., and
305 Stern, D.L. (2011). Multiplexed shotgun genotyping for rapid and efficient genetic mapping.
306 *Genome Res.* 21, 610–617.
- 307 32. Broman, K.W., and Sen, S. (2009). *A Guide to QTL Mapping with R/qlt* 1st ed. (Springer).
- 308 33. Broman, K.W., Wu, H., Sen, S., and Churchill, G.A. (2003). R/qlt: QTL mapping in
309 experimental crosses. *Bioinformatics* 19, 889–890.
- 310 34. Haley, C.S., and Knott, S.A. (1992). A simple regression method for mapping quantitative
311 trait loci in line crosses using flanking markers. *Heredity (Edinb)*. 69, 315–324.
- 312 35. Venken, K.J.T., Popodi, E., Holtzman, S.L., Schulze, K.L., Park, S., Carlson, J.W., Hoskins,
313 R.A., Bellen, H.J., and Kaufman, T.C. (2010). A molecularly defined duplication set for the X
314 chromosome of *Drosophila melanogaster*. *Genetics* 186, 1111–1125.
- 315 36. Turissini, D.A., McGirr, J.A., Patel, S.S., David, J.R., and Matute, D.R. (2017). The rate of
316 evolution of postmating-prezygotic reproductive isolation in *Drosophila*. *Mol. Biol. Evol.*
- 317 37. Schneider, C.A., Rasband, W.S., and Eliceiri, K.W. (2012). NIH Image to ImageJ: 25 years of
318 image analysis. *Nat. Methods* 9, 671–675.
- 319 38. Kvon, E.Z., Kazmar, T., Stampfel, G., Yáñez-Cuna, J.O., Pagani, M., Schernhuber, K.,
320 Dickson, B.J., and Stark, A. (2014). Genome-scale functional characterization of *Drosophila*
321 developmental enhancers in vivo. *Nature* 512, 91–95.
- 322 39. Taylor, B.J. (1989). Sexually dimorphic neurons in the terminalia of *Drosophila*
323 *melanogaster*: I. Development of sensory neurons in the genital disc during metamorphosis.
324 *J. Neurogenet.* 5, 173–192.
- 325 40. Dietzl, G., Chen, D., Schnorrer, F., Su, K.-C., Barinova, Y., Fellner, M., Gasser, B., Kinsey,
326 K., Oppel, S., Scheiblaue, S., *et al.* (2007). A genome-wide transgenic RNAi library for
327 conditional gene inactivation in *Drosophila*. *Nature* 448, 151–156.
- 328 41. Jenett, A., Rubin, G.M., Ngo, T.-T., Shepherd, D., Murphy, C., Dionne, H., Pfeiffer, B.D.,
329 Cavallaro, A., Hall, D., Jeter, J., *et al.* (2012). A GAL4-driver line resource for *Drosophila*
330 neurobiology. *Cell Rep.* 2, 991–1001.

- 331 42. Gibson, D.G., Young, L., Chuang, R.-Y., Venter, J.C., Hutchison, C.A., and Smith, H.O.
332 (2009). Enzymatic assembly of DNA molecules up to several hundred kilobases. *Nat.*
333 *Methods* 6, 343–345.
- 334 43. Bryne, J.C., Valen, E., Tang, M.-H.E., Marstrand, T., Winther, O., da Piedade, I., Krogh, A.,
335 Lenhard, B., and Sandelin, A. (2007). JASPAR, the open access database of transcription
336 factor-binding profiles: new content and tools in the 2008 update. *Nucleic Acids Res.* 36,
337 D102–D106.
- 338 44. Zhu, L.J., Christensen, R.G., Kazemian, M., Hull, C.J., Enuameh, M.S., Basciotta, M.D.,
339 Brasefield, J.A., Zhu, C., Asriyan, Y., Lapointe, D.S., *et al.* (2010). FlyFactorSurvey: a
340 database of *Drosophila* transcription factor binding specificities determined using the
341 bacterial one-hybrid system. *Nucleic Acids Res.* 39, D111–D117.
- 342 45. Culi, J., and Modolell, J. (1998). Proneural gene self-stimulation in neural precursors: an
343 essential mechanism for sense organ development that is regulated by Notch signaling. *Genes*
344 *Dev.* 12, 2036–2047.
- 345 46. Jeong, S., Rokas, A., and Carroll, S.B. (2006). Regulation of Body Pigmentation by the
346 Abdominal-B Hox Protein and Its Gain and Loss in *Drosophila* Evolution. *Cell*
347 125, 1387–1399.
- 348 47. Frangioni, J. V., and Neel, B.G. (1993). Solubilization and purification of enzymatically
349 active glutathione S-transferase (pGEX) fusion proteins. *Anal. Biochem.* 210, 179–187.
- 350 48. Fan, Y.-J., Gittis, A.H., Juge, F., Qiu, C., Xu, Y.-Z., and Rabinow, L. (2014). Multifunctional
351 RNA Processing Protein SRm160 Induces Apoptosis and Regulates Eye and Genital
352 Development in *Drosophila*. *Genetics* 197, 1251–1265.
- 353 49. Chatterjee, S.S., Uppendahl, L.D., Chowdhury, M.A., Ip, P.-L., and Siegal, M.L. (2011). The
354 female-specific Doublesex isoform regulates pleiotropic transcription factors to pattern
355 genital development in *Drosophila*. *Development* 138, 1099–1109.
- 356 50. Skaer, N., Pistillo, D., and Simpson, P. (2002). Transcriptional heterochrony of scute and
357 changes in bristle pattern between two closely related species of blowfly. *Dev. Biol.* 252, 31–
358 45.
- 359 51. Casanova, J., Sánchez-Herrero, E., and Morata, G. (1986). Identification and characterization
360 of a parasegment specific regulatory element of the abdominal-B gene of *Drosophila*. *Cell*
361 47, 627–636.
- 362 52. Hopmann, R., Duncan, D., and Duncan, I. (1995). Transvection in the *iab-5, 6, 7* region of
363 the *bithorax* complex of *Drosophila*: homology independent interactions in trans. *Genetics*
364 139, 815–833.
- 365 53. Xu, T., and Rubin, G.M. (1993). Analysis of genetic mosaics in developing and adult
366 *Drosophila* tissues. *Development* 117, 1223–1237.

- 367 54. Estrada, B., and Sánchez-Herrero, E. (2001). The Hox gene Abdominal-B antagonizes
368 appendage development in the genital disc of *Drosophila*. *Development* 128, 331–339.
- 369 55. Maroni, G., and Stamey, S.C. (1983). Developmental profile and tissue distribution of
370 alcohol dehydrogenase. *Drosoph. Inf. Serv.* 59.
- 371 56. Andres, A.J., and Thummel, C.S. (1994). Methods for quantitative analysis of transcription in
372 larvae and prepupae. *Methods Cell Biol.* 44, 565–573.
- 373 57. Crawley, M.J. (2012). *The R book* (John Wiley & Sons)
- 374 58. Hilbe, J.M. (2014). *Modeling Count Data* (Cambridge University Press).
- 375 59. Zuur, A., Ieno, E.N., Walker, N., Saveliev, A.A., and Smith, G.M. (2011). *Mixed Effects
376 Models and Extensions in Ecology with R Softcover.* (New York, NY: Springer).
- 377 60. Team, R.C. (2016). *R: A language and environment for statistical.*
- 378 61. Bates, D., Mächler, M., Bolker, B., and Walker, S. (2014). Fitting linear mixed-effects
379 models using lme4. *arXiv Prepr. arXiv1406.5823.*
- 380 62. Hothorn, T., Bretz, F., and Westfall, P. (2008). Simultaneous inference in general parametric
381 models. *Biometrical J.* 50, 346–363.
- 382 63. Bretz, F., Hothorn, T., and Westfall, P. (2010). *Multiple comparisons using R* (CRC Press).
- 383 64. Holm, S. (1979). A simple sequentially rejective multiple test procedure. *Scand. J. Stat.*, 65–
384 70.
- 65 Corson, F., Couturier, L., Rouault, H., Mazouni, K., & Schweisguth, F. (2017). Self-
organized Notch dynamics generate stereotyped sensory organ patterns in *Drosophila*.
Science, 356(6337), eaai7407.
66. Pfeiffer, B.D., Jenett, A., Hammonds, A.S., Ngo, T.-T.B., Misra, S., Murphy, C., Scully, A.,
Carlson, J.W., Wan, K.H., Laverty, T.R., et al. (2008). Tools for neuroanatomy and
neurogenetics in *Drosophila*. *Proc. Natl. Acad. Sci. U. S. A.* 105, 9715–9720.

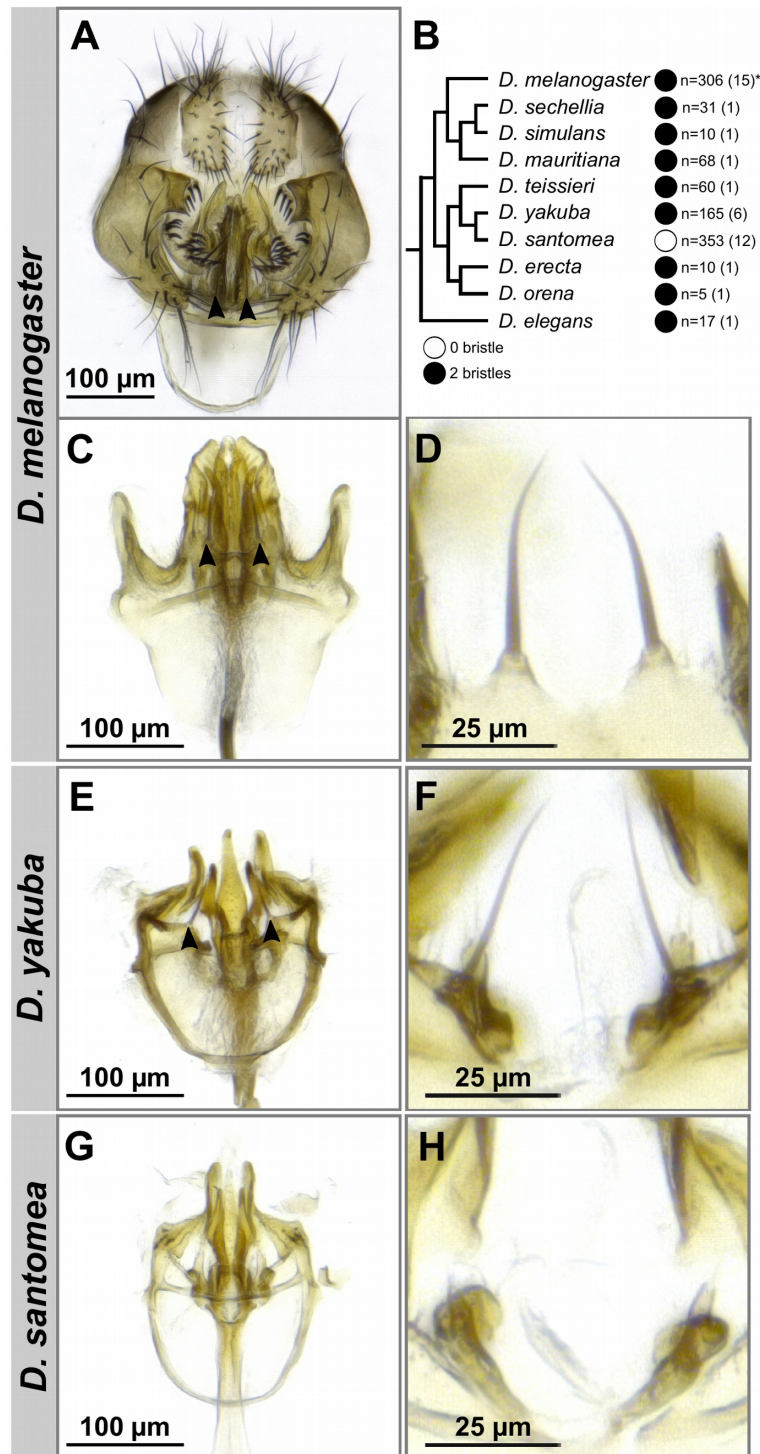
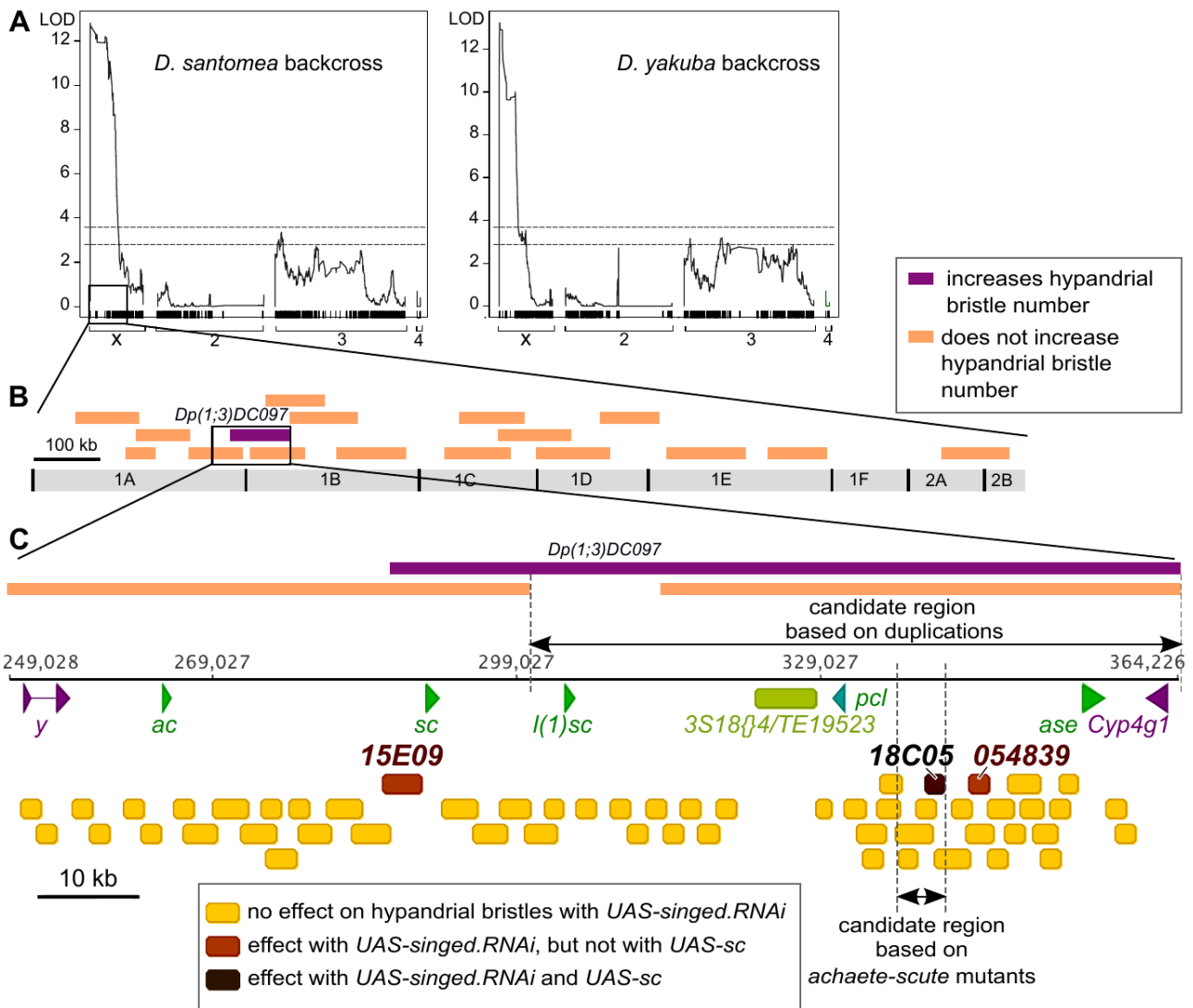
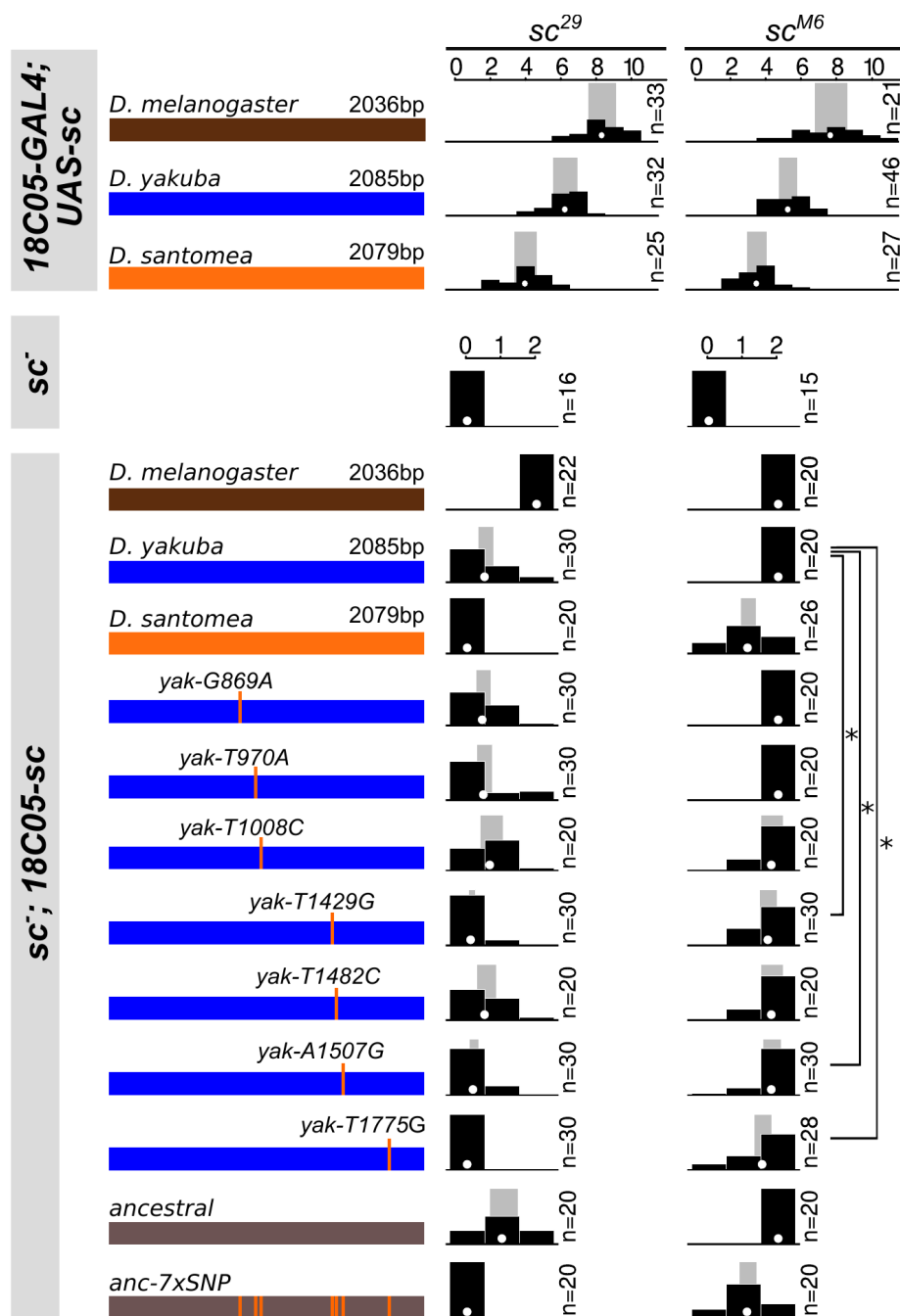


Figure 1. *D. santomea* lost hypandrial bristles.

(A) *Drosophila melanogaster* male genitalia. (B) Phylogeny of the *Drosophila melanogaster* species subgroup. All species of have two hypandrial bristles (black circles) except *Drosophila santomea*, which lacks hypandrial bristles (white circle). n: number of scored males, with the number of scored strains in parentheses. Asterisk indicates that 4 males out of 306 had three hypandrial bristles. (C-H) Light microscope preparations of ventral genitalia (C,E,G) and hypandrial bristles (D,F,H) in *D. melanogaster* (C-D), *D. yakuba* (E-F) and *D. santomea* (G-H). Hypandrial bristles are indicated with arrowheads on A, C and E.



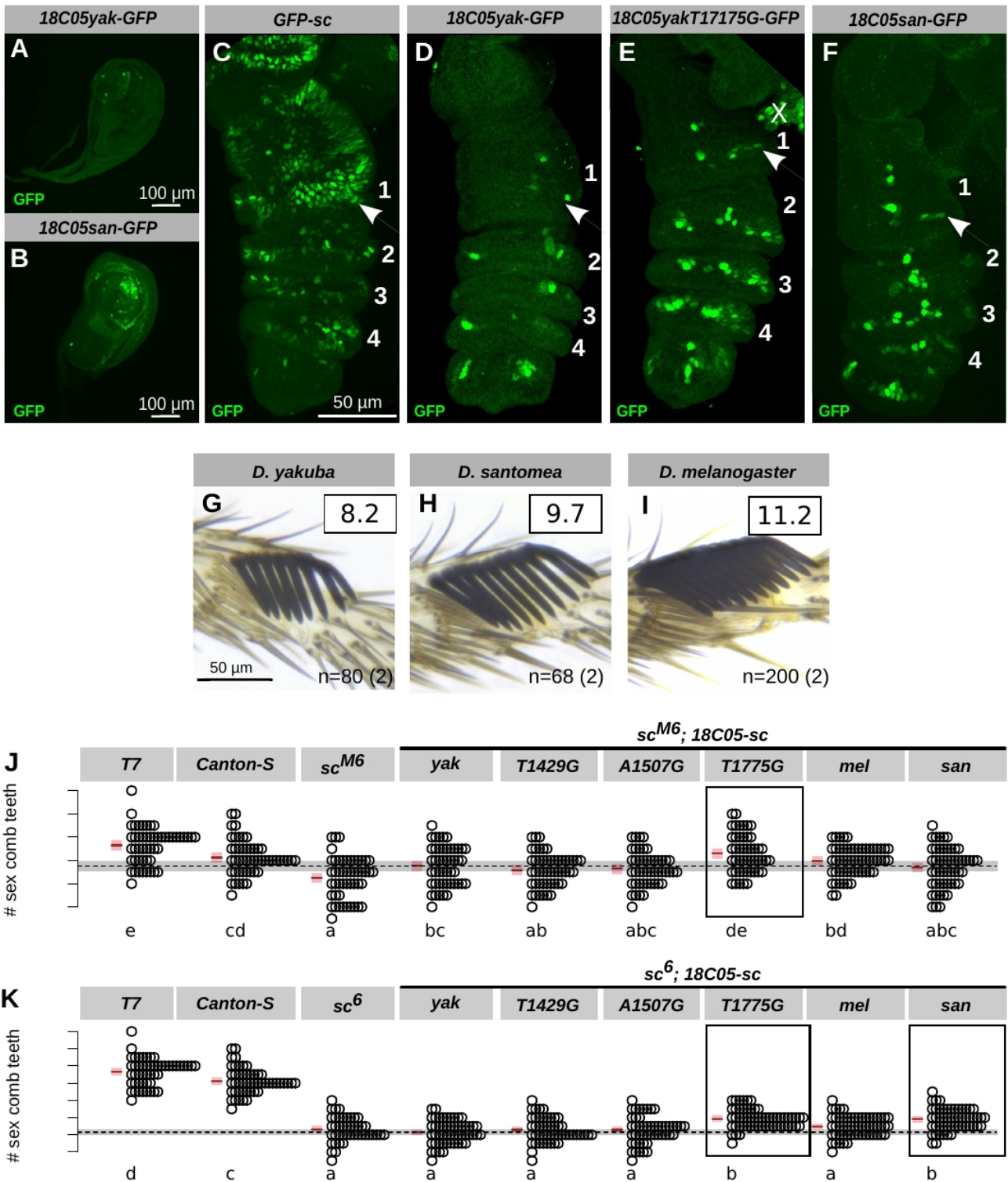
387 **Figure 2. Mapping of the cis-regulatory element involved in hypandrial bristle evolution.**
 388 (A) QTL analysis of hypandrial bristle number in a *D. santomea* backcross (left) and a *D. yakuba*
 389 backcross (right). On the y-axis are the LOD profiles from a Haley-Knott regression analysis. The
 390 x-axis represents physical map position in the *D. yakuba* genome. Ticks represent recombination
 391 informative markers. Dotted lines represent the 1% (top) and 5% (bottom) significance thresholds.
 392 (B) Schematic representation of the left tip of chromosome X and of 19 duplicated fragments of
 393 chromosome X that were tested for their effect on hypandrial bristle number in *D. santomea*-*D.*
 394 *melanogaster* hybrid males. All duplications had no significant effect (orange) except
 395 *Dp(1;3)DC097* (purple), which significantly increased hypandrial bristle number. (C) Genomic
 396 organization of the AS-C locus in *D. melanogaster*. Arrows indicate the coding regions of *yellow*
 397 (*y*), *achaete* (*a*), *scute* (*sc*), *lethal of scute* (*l(1)sc*), *pepsinogen-like* (*pcl*), *asense* (*ase*) and
 398 *cytochrome P450-4g1* (*Cyp4g1*) genes. The light green box represents the insertion of a
 399 *3S18{}/4/TF9523* natural transposable element. Boxes indicate cis-regulatory elements whose
 400 corresponding *GAL4* reporter lines have been tested. Expression of *UAS-singed.RNAi* with 52
 401 *GAL4* lines (yellow boxes) has no effect while it results in singed hypandrium bristles with *15E09*-,
 402 *18C05*- and *054839*-*GAL4*. Extra hypandrial bristles are found with *UAS-sc* and *18C05*-*GAL4*
 403 (dark brown box) but not with *15E09*- and *054839*-*GAL4* (light brown boxes).
 404



405
406
407
408
409
410
411
412
413
414
415
416
417
418
419

Figure 3. Three *D. santomea*-specific substitutions in *18C05* contribute to the loss of hypandrial bristles.

Rescue of the hypandrial bristle loss of *sc*²⁹ (left column) and *sc*^{M6} (right column) *D. melanogaster* mutants by expression of either *GAL4* with *UAS-sc* or *sc* driven by *18C05* sequences from *D. melanogaster* (brown), *D. yakuba* (blue) and *D. santomea* (orange). Seven *D. santomea*-specific substitutions (vertical orange bars) were introduced into either the *D. yakuba* region (blue) or the ancestrally reconstructed *18C05* region (grey). Distribution of hypandrial bristle number (black histogram), together with mean (white dot) and 95% confidence interval (grey rectangle) from a fitted GLM Quasi-Poisson model are shown for each genotype. Note that for a given rescue construct, *18C05-GAL4 UAS-sc* produces more hypandrial bristles than *18C05-sc*, probably due to the amplification of gene expression caused by the *GAL4/UAS* system. n: number of scored individuals. *: $p < 0.05$



420 **Figure 4. *D. santomea*-specific substitution *T1775G* contributes to increase in sex comb tooth**
 421 **number.**

422 (A-F) GFP staining (green) in T1 leg discs of late L3 larvae (A-B) and in 5h APF pupal legs (C-F)
 423 in *D. melanogaster* containing *18C05* reporter transgenes or *sc-GFP*. Genotype is indicated on top
 424 of each panel. Tarsal segments are numbered. Arrowheads point to the presumptive sex comb
 425 regions. “X” indicates non-leg tissue. (G-I) Leg sex comb in *D. yakuba* (G), *D. santomea* (H) and
 426 *D. melanogaster* (I). Average sex comb tooth numbers per leg are shown in squares. n: number of
 427 scored individuals, with the number of scored strains in parentheses. (J-K) Sex comb tooth number
 428 in wild-type (T7 and Canton-S), sc^{M6} (J) and sc^6 (K) mutants rescued with different *18C05-sc*

429 constructs. Each circle represents one male raised at 25°C. Mean (brown line) and 95% confidence
430 interval (pink rectangle) from a fitted GLM Quasi-Poisson model are shown. Letters indicate the
431 results of all-pairwise comparisons after Holm-Bonferroni correction. Two genotypes are
432 significantly different from each other ($p < 0.05$) when they do not share a letter. For easier
433 comparison, the horizontal dashed line and the surrounding grey line indicate the mean and 95%
434 confidence interval for *sc⁺;18C05yak-sc*. Transgenic constructs with sex comb tooth number
435 significantly different from *18C05yak-sc* are shown in boxes in J-K. On average *D. santomea* males
436 have about 1 extra tooth per sex comb compared to *D. yakuba* (G-H). The substitution *T1775G*
437 produces on average 0.5 extra sex comb tooth per leg, which is more than expected. It is possible
438 that the *D. melanogaster* background, where all our rescue constructs were tested, amplifies the
439 effect of the tested substitutions, especially since *D. melanogaster* males have more sex comb teeth
440 than *D. santomea* or *D. yakuba*.

441 STAR*METHODS

442

443 CONTACT FOR REAGENT AND RESOURCE SHARING

444 Further information and requests for resources and reagents should be directed to and will be
445 fulfilled by the Lead Contact, Virginie Courtier-Orgozo (virginie.courtier@normalesup.org).

446

447 EXPERIMENTAL MODEL AND SUBJECT DETAILS

448 The origin of all the fly strains used can be found in KRT Table, Table S1 and Extra Tables. All flies
449 were cultured on standard cornmeal–agar medium in uncrowded conditions at 25°C unless stated.
450 We used *Canton-S* as a wild-type *D. melanogaster* strain. Transgenic constructs were integrated into
451 the *attP2* landing site in *D. melanogaster* *w¹¹¹⁸* by BestGene Inc. Hybrid males between *D. yakuba*
452 and *D. santomea* were obtained by collecting 20 virgin females with 20 males from each stocks and
453 crossing them reciprocally in both directions. At least 10 such crosses were made and flipped every
454 4-5 days for several weeks. For QTL mapping, *D. yakuba* *yellow[1]* virgin females were crossed *en*
455 *masse* to *D. santomea* SYN2005 males to generate F1 hybrid females, which were subsequently
456 backcrossed, separately, to both parental strains. Genitalia of backcross males were isolated for
457 dissection and the remaining carcass was stored at -20 °C for subsequent sequencing library
458 preparation.

459

460

461 METHOD DETAILS

462

463 Genotyping of backcross males for QTL mapping

464 The carcass of each male was crushed in a 1.5-ml Eppendorf tube with a manual pestle in 180 µl of
465 Qiagen Tissue Lysis buffer. DNA of individual flies was extracted using Qiagen DNeasy Blood &
466 Tissue extraction kit (cat #69506). A Multiplexed Shotgun Genotyping sequencing library was made
467 from 189 *D. santomea* backcross males and for 181 *D. yakuba* backcross males as described
468 previously [31]. The list of barcodes used in this study can be found in Mendeley
469 (<http://dx.doi.org/10.17632/xjvz2m8z6r.1>) or in the Extra Data files, within the names of the
470 individuals that were sequenced. *D. yakuba* and *D. santomea* parental genome sequences were
471 generated by updating the *D. yakuba* genome sequence *dyak-4-chromosome-r1.3.fasta* with
472 Illumina paired-end reads from *D. yakuba* *yellow[1]* and *D. santomea* SYN2005 (sequenced by
473 BGI) using the *msgUpdateParentals.pl* function of the MSG software package. The resulting
474 updated genome files are *dsan-all-chromosome-yak1.3-r1.0.fasta.msg.updated.fasta* and *dyak-4-*
475 *chromosome-r1.3.fasta.msg.updated.fasta*. Ancestry was estimated for all backcross progeny using
476 MSG software (github.com/YourePrettyGood/msg). Ancestry files were reduced to only those
477 markers informative for recombination events using the script *pull_thin_tsv.py*
478 (github.com/dstern/pull_thin). Markers were considered informative when the conditional
479 probability of being homozygous differed by more than 0.05 from their neighboring markers.

480

481 QTL mapping

482 QTL mapping was performed using the R/*qtl* package version 1.4 [32,33]. The thinned posterior
483 genotype probabilities were imported into R/*qtl* using the R function *read.cross.msg.1.5.R*
484 (github.com/dstern/read_cross_msg). QTL mapping was performed independently on each
485 backcross population. We performed genome scans with a single QTL model (“scanone”) using the

486 Haley-Knott regression method [34] which performs well with genotype information at a large
487 number of positions along the genome. The genome-wide 5% and 1% significance levels were
488 determined using 1,000 permutations. One QTL peak above the 1% significance level was found for
489 both backcrosses. To check for additional QTL, we built a QTL model with this single QTL using
490 the “fitqtl” function and scanned for additional QTL using the “addqtl” function. A second QTL was
491 found on chromosome 3 for both backcrosses. When introduced into a new multiple QTL model,
492 refined and fitted to account for possible interactions, a third significant QTL was found. Based on
493 the full three-QTL model, no additional significant QTL were found with the function “addqtl”: the
494 highest LOD score for a fourth QTL reached only 1.8 and 1.2 for the *D. yakuba* backcross and the
495 *D. santomea* backcross, respectively. Various three-QTL models with different interactions between
496 loci were assessed. Positive significant interaction was detected between the QTL on chromosome 1
497 and both QTLs on chromosome 3. The interaction between the two QTLs on chromosome 3 was
498 not significant. For the three-QTL model with interactions between the QTL on chromosome 1 and
499 both QTLs on chromosome 3, we computed the LOD score of the full model and the estimated
500 effects of each locus. The 2-LOD intervals were calculated using the “lodint” function with
501 parameter drop of 2. Analysis of F1 hybrid males is consistent with a large effect of the X
502 chromosome on hypandrial bristle number: male F1 hybrids carrying a *D. yakuba* X chromosome
503 have on average 1.9 hypandrial bristles (n=34) while reciprocal hybrid males possessing the *D.*
504 *santomea* X chromosome have none (n=29) (Extra Tables). Note that few informative markers are
505 found on the right arm of chromosome 2, suggesting the presence of an inversion between parental
506 lines. In both backcrosses the large-effect QTL is estimated to cause a decrease of 0.9 ± 0.1 bristles
507 between a *D. yakuba* hemizygote and a *D. santomea* hemizygote male (Extra Data Files). The QTL
508 peak is at position 46,886 and 221,928 for the *D. santomea* and *D. yakuba* backcross, respectively.
509 The AS-C locus is at position 179,000-290,000.

510

511 Duplication Mapping in *D. santomea*-*D. melanogaster* hybrids

512 We used a set of *D. melanogaster* duplication lines to test overlapping parts of chromosome X for
513 their effect on hypandrial bristle number [35]. Each line contains a fragment of the chromosome X
514 inserted into the same attP docking site on chromosome 3L using Φ C31 integrase, allowing direct
515 comparison between fragments. Each duplication was used to screen for complementation of the
516 loss of function allele(s) from *D. santomea*. We exploited the fact that rare *D. santomea*-*D.*
517 *melanogaster* hybrid males can be produced by crossing *D. melanogaster* females carrying a
518 compound X chromosome with *D. santomea* males [36]. The resulting hybrid males carry a *D.*
519 *santomea* X chromosome. We first created a *D. melanogaster* stock whose genotype is *TM3, Sb[1]*
520 *Ser[1]/Nup98-96[339]* by crossing *Nup98-96[339]/TM3, Sb[1]* with *Df(3R)D605/TM3, Sb[1]*
521 *Ser[1]*. We then performed three successive crosses at room temperature in glass vials: (a) *C(1)RM,*
522 *y[1] w[1] f[1] ; +/+ \times +/+; TM3, Sb[1] Ser[1]/Nup98-96[339]*, (b) *C(1)RM, y[1] w[1] f[1] ; TM3,*
523 *Sb[1] Ser[1]/+ \times +/Y; Dp(1,3)/Dp(1,3)*, (c) *C(1)RM, y[1] w[1] f[1] ; TM3, Sb[1] Ser[1]/Dp(1,3)*
524 *D. melanogaster* females \times *D. santomea* males. The same procedure was followed for 21
525 duplication lines and progeny was obtained for 17 of them. Hybrid males from the last cross were
526 sorted in two pools, the [*Sb*⁻, *Ser*⁻] males who carried the duplication and the [*Sb*⁺, *Ser*⁺] males
527 which were used as controls which carried no duplication but the balancer chromosome *TM3 Sb[1]*
528 *Ser[1]*. In *D. melanogaster*/*D. santomea* hybrids, dominant markers are not always fully penetrant.
529 A few progeny males exhibited [*Sb*⁺, *Ser*⁻] or [*Sb*⁻, *Ser*⁺] phenotypes; they were considered as
530 control individuals carrying the balancer chromosome *TM3, Sb[1] Ser[1]*. Males were stored in
531 ethanol until dissection. Duplication mapping narrowed down the causal region to a 84.6 kb region
532 (*DC097*) of the *achaete-scute* complex (AS-C) (Figure 2.B-C, see also Extra Tables, GLM-Poisson,
533 $\text{Chisq}(17,478)=398.44$, $p = 10^{-4}$).

534

535 Examination of Hypandrial Bristle Phenotypes

536 Male genitalia were cut with forceps and then hypandria were dissected with fine needles or forceps
537 Dumont #5 (112525-20, Phymep) in a drop of 1x PBS. For *D. melanogaster* in order to see the
538 hypandrial bristles better we removed the aedeagus by holding the aedeagal apodem with forceps
539 and gently pushing the hypandrium upwards with an other forceps until it separated. Hypandria
540 were mounted in DMHF (Dimethyl Hydantoin Formaldehyde, Entomopraxis). Before dissection,
541 males were sometimes stored at -20°C in empty Eppendorf tubes or in glycerol:acetate:ethanol
542 (1:1:3) solution. For analysis of non-hypandrial bristles, males were stored at -20°C in
543 glycerol:acetate:ethanol (1:1:3) solution. We never stored these males in empty tubes because we
544 found that such a storage procedure can break and remove external bristles (but, as far as we know,
545 hypandrial bristles were not affected by such a procedure, maybe because hypandrial bristles are
546 relatively internal and protected by the epandrium). Furthermore, we never observed a single socket
547 devoid of shaft on the male hypandrium, indicating that hypandrial bristles cannot be accidentally
548 cut or lost with our experimental protocol. 3D projection images of the preparations were taken at
549 500X magnification with the Keyence digital microscope VHX 2000 using optical zoom lens VH-
550 Z20R/W.

551

552 Examination of Other Bristles

553 Since genitalia are the most rapidly evolving organs in animals with internal fertilization [26], we
554 compared the number of genital bristles between two strains of *D. yakuba* and two strains of *D.*
555 *santomea*. We found no difference between *D. yakuba* and *D. santomea* in any genital bristles
556 except for anal plate and clasper bristles, where a slightly significant interspecific variation was
557 detected (Extra Figures). The loss of hypandrial bristles in *D. santomea* is thus the major change in
558 genital bristles between *D. santomea* and *D. yakuba*. Genitalia were dissected in 1X PBS, hypandria
559 were removed and the epandria were mounted in 99% glycerol. Gentle pressure was applied on the
560 cover-slip with forceps to flatten the preparations in order to see all bristles. Pictures were taken at a
561 500X magnification with a digital microscope VHX 2000 (Keyence) using lens VH-Z20R/W.
562 Bristles were counted on the images.

563 For sex comb preparations, prothoracic legs were dissected at the coxa with forceps Dumont #5 and
564 were mounted in DMHF (Dimethyl Hydantoin Formaldehyde, Entomopraxis). Images of the sex
565 combs were taken at 1000x magnification with the Keyence digital microscope as written above.
566 Sex comb teeth were counted on the images with Image J [37].

567

568 Analysis of *scute* coding sequence

569 The *scute* coding sequence (CDS) of *D. melanogaster* iso-1 was retrieved from FlyBase. We
570 blasted the updated genome sequences of *D. yakuba* yellow[1] and *D. santomea* SYN2005 (see
571 above) with *D. melanogaster* *scute* coding region and retrieved only one locus in each species. The
572 *scute* coding region was then annotated with Geneious and no intron was found, as in *D.*
573 *melanogaster*.

574

575 Screening *as-GAL4* lines for expression in the hypandrium

576 The *as-GAL4* lines were ordered from VDRC [38] and Bloomington Stock Center (Extra Tables).
577 Two lines were not available (*GMR1509* and *VT054822*) so we created new transgenic lines for
578 these regions, named *GMR15X09-GAL4* and *VT054822b-GAL4* (see below). Because screens are
579 easier on adults than on genital discs, and also because the exact developmental stage and location
580 of hypandrial bristle development are unknown [39], we decided to look for GAL4-triggered
581 phenotypes in adult males. As a readout of GAL4 expression, we tested various UAS lines (*UAS-*
582 *mCD8-GFP*, *UAS-yellow* in a yellow mutant background, *UAS-sc.RNAi*, *UAS-achaete.RNAi*, *UAS-*
583 *forked.RNAi*, *UAS-singed.RNAi*) (lines are listed in KRT Table, see also Extra Tables) together
584 with *DC-GAL4*, which drives expression in the dorso-central thoracic bristles [40]. To enhance
585 RNAi potency we also used *UAS-Dicer-2* [40]. With *UAS-mCD8-GFP* and *UAS-yellow* the change

586 in fluorescence or color was hardly visible. The most penetrant bristle phenotype was obtained with
587 *UAS-Dicer-2 UAS-singed.RNAi¹⁰⁵⁷⁴⁷* at 29 °C (Extra Tables). Therefore this line was chosen for
588 screening all the *as-GAL4* constructs.

589 Five *as-GAL4* males of each *as-GAL4* line were crossed to five *Dcr2; UAS-*
590 *singed¹⁰⁵⁷⁴⁷.RNAi/CyO* virgin females. Crosses were kept at 29 °C. The non-curly males (*Dcr2;*
591 *UAS-singed¹⁰⁵⁷⁴⁷.RNAi/+; +/-as-GAL4*) were collected for dissection and kept at -20 °C. Hypandrium
592 dissection and image acquisition were performed as indicated above. For each *as-GAL4* line at least
593 5 genitalia were examined (Extra Tables).

594 To test whether the *15E09*, *18C05* and *054839* enhancer-*GAL4* drive expression in the
595 hypandrial bristle region in absence of *sc*, we crossed five *sc²⁹; UAS-scute (III)* females with five
596 males of each respective *GAL4* line, as well as five *sc^{M6}/FM7 ; UAS-scute (III)* females with five
597 males of each respective *GAL4* line. Of the three *GAL4* lines, only *18C05* could induce hypandrial
598 bristles with *UAS-sc* in a *sc* mutant background. The *18C05-GAL4* line produced approximately 10
599 bristles, where normally only two develop, which may reflect the amplification of gene expression
600 that is inherent to the *UAS-GAL4* system. These results suggest that only *18C05* drives sufficiently
601 strong expression in the hypandrial region to alter bristle patterning.

602

603 Cloning of enhancers into pBPGUw and pBPSUw

604 Enhancers were cloned into the *GAL4* reporter vector pBPGUw using the same strategy as
605 in [38,41]. Enhancer sequences were amplified by Phusion® High Fidelity Polymerase (New
606 England Biolabs) in two steps reaction using the primers and templates (Extra Tables). PCR
607 products and vectors were purified by Nucleospin Gel and PCR Clean-Up Kit (Machery-Nagel).
608 Clones were purified by E.Z.N.A.® Plasmid Mini Kit I (Omega Bio-tek). All *GAL4* constructs were
609 cloned using the Gateway® system (ThermoFisher Scientific). The enhancer fragments were first
610 ligated into *KpnI* and *HindIII* restriction enzyme site of the vector pENTR/D-TOPO (Addgene)
611 (Extra Tables). Recombination into the destination vector pBPGUw was performed using LR
612 clonase II enzyme mix (Invitrogen) and products were transformed into One Shot® TOP10
613 (Invitrogen) competent cells. Recombinant clones were selected by ampicillin resistance on Amp-
614 LB plates (100 µg/ml)

615 The pBPSUw vector was constructed by replacing the *GAL4* cassette of pBPGUw by *scute*
616 CDS. The *scute* CDS was amplified from *D. melanogaster iso-1* with Scute-CDS-Rev and Scute-
617 CDS-For primers and ligated into pGEM-T Easy (Promega). The *sc-CDS* insert was cut out using
618 *KpnI* and *HindIII* and cloned into *KpnI* and *HindIII* sites in pBPGUw, thus replacing *GAL4*. The
619 vector was named pBPSUw where “S” stands for *scute*. *18C05* sequences from *D. melanogaster*, *D*
620 *yakuba* and *D. santomea* were cloned into pBPSUw and tested in rescuing hypandrial bristles in *sc*
621 mutants as written above. We found that *18C05* from *D. melanogaster* rescued two hypandrial
622 bristles in both *sc²⁹* and *sc^{M6}* mutants. *D. santomea 18C05* enhancer rescued fewer hypandrial
623 bristles on average than the *D. yakuba 18C05* region (Figure 3., bristle number for *D. yakuba*
624 *18C05* in *sc²⁹* is significantly different from 0 (Exact-Poisson, $p < 10^{-16}$) and bristle number for *D.*
625 *santomea 18C05* in *sc^{M6}* is significantly different from 2 (Exact-Poisson, $p = 0.0008$)).

626 The *18C05* full length sequences were amplified by PCR from *D. melanogaster iso-1* (BL2057), *D.*
627 *melanogaster T-7*, *D. yakuba Ivory Coast* and *D. santomea SYN2005* with the primers described in
628 Extra Tables. The PCR products were cloned into pBPSUw as described above. Three different *D.*
629 *melanogaster 18C05* sequences were tested with *UAS-sc* in the hypandrium in *sc²⁹* and *sc^{M6}*. *GMR-*
630 *18C05* (BL2057) was obtained from the Janelia Farm collection [41] and *18C05_BL2057* and
631 *18C05_T7* were cloned in this study. Hypandrial bristle number was found to be significantly
632 higher for *GMR-18C05* than for *18C05_BL2057* and *18C05_T7* in both backgrounds (GLM-Quasi-
633 Poisson, $F(2, 63) = 16.88$, both $p < 10^{-6}$ for *sc²⁹*; $F(2, 58) = 20.9$, $p < 10^{-10}$ and $p < 10^{-5}$ for *sc^{M6}*).

634 The *GMR-18C05* fragment is inserted in the expression vector 3'-5' compared to the *D.*
635 *melanogaster* genome sequence. In contrast, the *18C05_BL2057* and *18C05_T7* are cloned 5'-3'. All

636 the *18C05* constructs we made were inserted in the same orientation, 5'-3'. *GMR-18C05* and
637 *18C05_BL2057* are the same sequences (from *D. melanogaster* Bloomington Stock Center Strain
638 #2057), but cloned in opposite directions. *18C05_T7* contains the *18C05* sequence of *D.*
639 *melanogaster T.7* strain. Comparing bristle number between *GMR-18C05-GAL4* and
640 *18C05_BL2057-GAL4* shows that the orientation of the cis-regulatory region has an effect on bristle
641 number.

642 The *18C05-chimera-pBPSUw* constructs were cloned using Gibson Assembly [42] by fusing
643 together different lengths of *18C05* sequences from *D. yakuba Ivory Coast* and *D. santomea*
644 *SYN2005*. The different chimeras are described in Extra Tables. Cloning primers were designed
645 using NEBuilder Tools (<http://nebuilder.neb.com/>). Primer sequences and templates used in PCR
646 are listed at Extra Tables. To assemble the *18C05* fragments in pBPSUw (Extra Tables), the vector
647 was linearized by *AatII* and *FseI* restriction enzymes (New England Biolabs Inc.). After digestion
648 thermosensitive alkaline phosphatase (FastAP, ThermoFisher Scientific) was added to the reaction
649 to prevent self-ligation of the plasmid. PCR products and the linearized plasmid were isolated from
650 1% agarose gels and spin column purified. Gibson Assembly was performed as in [42], except that
651 the assembly reactions were incubated at 37 °C for 10 minutes and then 3 hours at 50 °C in a PCR
652 machine. 2 µl of assembly mixtures were transformed into NEB® 10-beta (New England Biolabs
653 Inc.) competent cells and ampicillin-resistant colonies were selected on 100 µg/ml Amp-LB plates.
654 The Gibson Assembly Master-mix was prepared according to [42], its components were purchased
655 from Sigma-Aldrich.

656 The *18C05-yakubaSNP-pBPSUw* constructs were cloned by Gibson Assembly as described
657 above, except for *18C05yakT1008C* and *18C05yakT1482C* sequences, which were synthesized and
658 cloned by GenScript® (Extra Tables). The *18C05-ancestral* sequences were synthesized and cloned
659 by GenScript® into pBPSUw *AatII* and *FseI* sites, except for the *18C05_AncG869A*,
660 *18C05_AncT670G* and *18C05_Anc-7SNP* sequences, which were cloned by us by Gibson Assembly
661 into pBPSUw *AatII* and *FseI* sites using the *18C05_Ancestral_Gibson_forward* and
662 *18C05_Ancestral_Gibson_reverse* primers (Extra Tables).

663 All transgenic constructs were integrated into the *attP2* landing site in *D. melanogaster w¹¹¹⁸* by
664 BestGene Inc. The *T1775G* substitution affects nucleotide position 447,055 in the Dm6 reference
665 assembly.

666 Genomic DNA preparations for sequencing the *18C05* region

667 Genomic DNA was isolated with Zymo Research Quick-DNA™ Miniprep Plus Kit from 3
668 males and 3 females from the *D. yakuba*, *D. santomea* and *D. teissleri* lines listed in the summary of
669 the alignment of *18C05* sequences available at <https://doi.org/10.6084/m9.figshare.6972707>. *18C05*
670 sequences were amplified with San-Yak_lines_sequencing-For and San-Yak_lines_sequencing-Rev
671 primers (Extra Figures) using Phusion® High Fidelity Polymerase (New England Biolabs).
672

673 Sequence Analysis

674 Geneious software was used for cloning design and DNA sequence analysis. Nucleotide positions
675 are given according to the alignment of *D. yakuba Ivory Coast 18C05* sequence with *D. santomea*
676 *SYN2005 18C05* sequence. The *18C05ancestral* sequence of *D. yakuba* and *D. santomea* was
677 reconstructed in Geneious based on the *18C05* sequence alignment of multiple *Drosophila* species
678 available at <https://doi.org/10.6084/m9.figshare.6972707>. Manual parsimony reconstruction of all
679 the ancestral nucleotides was unambiguous, except for one position (766, indel polymorphism),
680 where the sequence is absent in the *simulans* complex and in *D. santomea*, while it is present in *D.*
681 *teissleri* and polymorphic in *D. yakuba*. For this position we chose *D. teissleri* as the ancestral
682 sequence. The *18C05* sequences of *D. melanogaster* subgroup species were retrieved by BLAST
683 from the NCBI website. Transcription Factor (TF) binding sites in *18C05* were predicted using the
684 JASPAR CORE Insecta database (<http://jaspar.genereg.net> [43]). 25-60 bp sequences of *18C05*
685

686 were scanned with all JASPAR matrix models with 50-95% Relative Profile Score Thresholds to
687 test for sensitivity and selectivity [43] (Table S3). For TFs which were absent in JASPAR (Scute),
688 we used Fly Factor Survey [44] to analyze their putative binding affinities to the probe. As *sc* cis-
689 regulatory region is known to contain binding sites for Scute itself [45], we looked for Scute
690 binding sites in *18C05*, *15E09* and *054839*. Two putative Scute binding sites (consensus motif
691 *CAYCTGY*, Fly Factor Survey [44] were found in *15E09* and *054839* but not in *18C05*. Given the
692 present results, we cannot exclude the involvement of *15E09* and *054839* in the evolution of
693 hypandrial bristle evolution in *D. santomea*. In this paper, we decided to focus on the *18C05*
694 enhancer, whose effect could be studied in a *sc* mutant background.

695

696 Abd-B homeodomain (Abd-B-HD) purification and EMSA

697 The Abd-B-HD-pGEX-4T-1 plasmid [46] (kindly provided by Sangyun Jeong) was transformed
698 into BL21 (DE3) chemically competent cells. Protein expression was induced by 0.1 mM IPTG
699 (isopropyl- β -D-thiogalactopyranoside, Sigma Aldrich). Recombinant protein was purified from 500
700 ml of bacterial culture as described in Frangioni [47] except that proteins were eluted into 50 mM
701 Tris-HCl, pH 8.0, 500 mM NaCl, 10mM reduced glutation (Sigma-Aldrich, G-4251) and 5%
702 glycerol. Concentrations and purity of the protein were determined by SDS-PAGE and Qubit 2.0
703 Fluorometer (Life Technologies). Protein aliquots of 20 μ l were snap-frozen in liquid nitrogen and
704 stored at -80 °C.

705 The HPLC-purified biotinylated and non-labelled oligonucleotides (Sigma-Aldrich) were used
706 in PCR to obtain 54 bp probes *yak* and *san* (*san=yakT1775G*) from *18C05yak-pBPSUw* and
707 *18C05yakT1775G-pBPSUw* plasmid templates. Oligonucleotides are listed in Extra Tables. PCR
708 products were column-purified.

709 We then used electrophoretic mobility shift assay (EMSA) to test whether the purified Abd-B
710 homeodomain (ABD-B-HD) can bind directly to a 54-bp fragment of *18C05* with the T1775G site
711 at position 13 containing either T (*yak* probe) or G (*san* probe). In each binding reaction, 20 fmol of
712 probes were mixed with the purified ABD-B HD ranging from 0-1.25 μ g (0 μ g, 0.75 μ g, 1 μ g and
713 1.25 μ g) in binding buffer containing 10mM TRIS pH 7.5, 50 mM KCl, 0.5 mM DTT, 6.25 mM
714 MgCl₂, 0.05 mM EDTA, 50 ng/ μ l Salmon Sperm DNA (Sigma Aldrich) and 9.00% Ficoll 400
715 (Sigma Aldrich). The competition assay was performed by adding 9 pmol of unlabeled probes (450-
716 fold excess) to the binding reaction. The reaction mixtures were incubated at 22 °C for 30 min and
717 run on a non-denaturing 6% polyacrylamide gel (Invitrogen) in 0.5X TBE (Eurofins).

718 Labeling reactions were carried out with LightShift™ Chemiluminiscent EMSA Kit
719 (ThermoFisher Scientific) according to the provider instructions with the following modifications:
720 after electrophoresis, gels were blotted overnight in 20X SSC using the TurboBlotter Kit (GE
721 Healthcare Life Sciences) and cross-linking of the probe to the membrane UV-light was performed
722 at 254 nm and 120 mJ/cm² (UV stratalinker® 2400, STRATAGENE). Chemiluminescence stained
723 membranes were exposed to a CDD camera (FUJIFILM, LAS-4000) for 50x 10 sec exposition time
724 increments. The last images were used for quantification and were never saturated according to
725 LAS 4000 software.

726 To quantify the binding affinity of Abd-B-HD to the probes, the fractional occupancy (ratio of
727 bound/(free+bound) probe) was calculated for three replicate experiments (Figure S4E) using the
728 intensity values of the bands measured in ImageJ [37]. The mean fractional occupancy was
729 significantly lower with *D. santomea* probes than with *D. yakuba* probes (ANCOVA,
730 $F(1,15)=10.58$, $p = 0.005$). We found that ABD-B-HD binds both *D. yakuba* and *D. santomea* DNA
731 (Figure S4B-D). ABD-B-HD binding to the *D. yakuba* probe always resulted in a stronger shift than
732 to the *D. santomea* probe. Furthermore, the *D. santomea* cold probe did not compete as efficiently
733 as the *D. yakuba* cold probe to prevent formation of the *D. yakuba* DNA-ABD-B-HD complex (U-
734 test, $p=0.05$).

735

736 Abd-B RNAi and clonal analysis

737 To test whether *Abd-B* is required for hypandrial bristle development, we reduced *Abd-B* expression
738 using either genetic mutations or RNAi. Two *UAS.Abd-B-RNAi* lines (#51167 and #26746) were
739 crossed with 3 different *GAL4* lines, *GMR18C05-GAL4*, *NP5130-GAL4* and *NP6333-GAL4*.
740 Crosses were kept at 29 °C and the hypandrium phenotype was examined in 10-50 F1 males (Table
741 S4). Using the genitalia *GAL4* drivers *esg-GAL4^{NP5130}* [48] and *NP6333* [49] to express *Abd-*
742 *B.RNAi⁵¹¹⁶⁷*, we obtained 20 males out of 100 with developed hypandrium, among which two
743 aberrant hypandrial bristle phenotypes were found, either bristle size reduction or bristle loss
744 (Figure S3A-F, n=9/11 for *NP5130*, n=8/9 for *NP6333*, Table S4). Smaller bristles might arise from
745 a delay in *sc* expression during development [50]. Since *Abd-B* null mutations are lethal [51], we
746 produced mitotic mutant clones for two null mutations, *Abd-B^{M1}* [51] and *Abd-B^{D18}* [52]. *Abd-B*
747 mutant mitotic recombinant clones were induced by the FLP/FRT system [53] using *Abd-B^{M1}* and
748 *Abd-B^{D18}* null mutations. To induce clones, ten *yw hsflp122; FRT82B hs-CD2 y⁺ M(3) w¹²³/TM2*
749 virgin females were crossed to ten *y; FRT82B Abd-B^{M1} red[1] e[11] ro[1] ca[1]/TM6B* or *y;*
750 *FRT82B Abd-B^{D18}/TM3* males (stocks were kindly provided by Ernesto Sánchez-Herrero). Crosses
751 were flipped every 24 hours and F1 progeny were heat-shocked at 38 °C for 1 hour at different
752 stages of larval development: 24-48, 48-72, 72-98 and 96-120 hours after egg laying [54]. From
753 both crosses, a total of 82 F1 males (Table 4) with the genotype of *yw hsflp122; FRT82B hs-CD2 y⁺*
754 *M(3) w¹²³/FRT82B Abd-B^{M1} red[1] e[11] ro[1] ca[1]* and *yw hsflp122; FRT82B hs-CD2 y⁺ M(3)*
755 *w¹²³/FRT82B Abd-B^{D18}* were examined. Hypandria were mounted and bristle clones were screened
756 as described above. Most of the resulting males showed extreme transformation of the genitalia
757 (Figure S4G-H, O-P) but 12 males out of 82 had analyzable hypandrium (twelve males for *Abd-B^{M1}*
758 and two males for *Abd-B^{D18}*). Among them, 6 males were devoid of one or both hypandrial bristles
759 (Figure S4I-N, Table S4). When hypandrial bristles were present, most of them were heterozygous
760 for the *Abd-B* mutation according to the visible markers associated with somatic recombination.
761 Together, our results suggest that *Abd-B* is required for hypandrial bristle development.

762

763 Immunostaining

764 For leg disc stainings the larvae were fed on freshly prepared Formula 4-24[®] Instant Drosophila
765 Medium, Blue (Carolina) and staged by the presence of blue staining in their gut [55]. Larvae were
766 chosen with the most clear gut, indicating a developmental stage of 1-6 hours before pupa formation
767 [56]. Head parts of the larvae were cut and fixed in 4% PFA in PBS pH 7.4 for 20 minutes at room
768 temperature. For pupal leg preparations the anterior part of the pupae were cut and fixed in 4% PFA
769 in PBS pH 7.4 for 50 minutes at room temperature. Following fixation, samples were washed three
770 times for 5 minutes in PBS containing 0.1% Tween20 and then permeabilized in TNT buffer (TRIS-
771 NaCl buffer containing 0.5% Triton X-100) for 10 minutes. Samples were washed in 5% BSA in
772 TNT for up to 5 hours at room temperature and then incubated with rabbit anti-GFP primary
773 antibodies (Thermofisher #A6455) diluted in 1:1000 in TNT overnight at 4 °C and rinsed in TNT
774 three times for 10 minutes at room temperature. Then, samples were washed in 5% BSA in TNT for
775 up to 5 hours at room temperature and incubated with donkey Anti-Rabbit Dylight[®] 488
776 (Thermofisher) secondary antibodies diluted 1:200 in TNT overnight at 4 °C. After washing the
777 preparations in TNT for 5 minutes DNA was stained in 1µg/µl DAPI solution (Sigma-Aldrich) for
778 30 minutes at room temperature. The preparations were finally washed in TNT three times for 5
779 minutes and the imaginal discs and pupal legs were dissected in PBS and mounted in Vectashield[®]
780 H-1000. Images were acquired using Spinning Disc CSU-W1. Number of GFP-positive cells were
781 counted in the z-stack using ImageJ [37] in a blind fashion regarding the genotypes using
782 randomized file names.

783

784 **QUANTIFICATION AND STATISTICAL ANALYSIS**

785

786 Since bristle number is a classical type of count data, we performed statistical analysis using
787 generalized linear models (GLM) and generalized linear mixed models (GLMM) where bristle
788 number, the response variable, is assumed to follow a Poisson distribution [57–59]. All statistical
789 analyses were performed using R 3.4 [60]. GLM were fitted with the function `glm()` ("stats" core
790 package 3.5.0) and GLMM with the function `glmer()` ("lme4" package 1.1-14 [61] with the
791 parameter "family" taken to be "Poisson". We tested differences in bristle number by comparing two
792 wild-type stocks of *D. yakuba* with two wild-type stocks of *D. santomea*. We tested the difference
793 between species, using a GLMM of the Poisson type (GLMM-Poisson) where the number of
794 bristles was the response variable, species was a fixed effect to test and stock a random effect. For
795 all other analyses, we tested differences in bristle number between genotypes using GLM of the
796 Poisson type (GLM-Poisson) where the response variable was bristle number and genotype, a
797 categorical variable, was the fixed effect. When we noticed important differences between residual
798 deviance and residual degrees of freedom, we also fitted a quasi-likelihood model of the type
799 "quasi-Poisson" (GLM-Quasi-Poisson) which allows for a model of the Poisson type, but where the
800 variance can differ from the mean and is estimated based on a dispersion parameter (see for
801 example [59] p. 225). For each model, in order to retain the model that fitted best to the data,
802 analysis of deviance was performed using the `anova.glm()` with "test = Chisq" for GLM-Poisson
803 and "test = F" for GLM-Quasi-Poisson. When needed, we performed multiple comparisons using
804 the `glht()` function and the "Holm" adjustment parameter ("multcomp" package 1.4-7 [62]) which
805 performs multiple comparisons between fitted GLM parameters and yields adjusted p-values
806 corrected according to the Holm-Bonferroni method [63,64] also performed an exact Poisson test (R
807 function "poisson.test") to test sample mean to a reference value assuming a Poisson distribution.
808 Mean and 95% confidence intervals were directly extracted from the fitted GLM and transformed
809 using `exp(coef())` and `exp(confint.default())`.

810 For EMSA data, response curves were compared between yak probe and san probe using an
811 ANCOVA after natural log transformation. The unlabeled san 450x responses were compared
812 between yak probe and san probe using a one-sided Mann-Whitney U-test.

813

814 DATA AVAILABILITY

815 Sequences were deposited into GenBank (accession numbers MG460736-MG460765). Source data
816 for Bristle Number, QTL mapping analysis, EMSA and immunostaining are available in BioRxiv
817 and at Mendeley: <http://dx.doi.org/10.17632/xjvz2m8z6r.1>. Additional Data Figures and Data
818 Tables are available in BioRxiv and at Figshare: <https://doi.org/10.6084/m9.figshare.6972707> and
819 <https://doi.org/10.6084/m9.figshare.6972740>, respectively.

820

821

REAGENT or RESOURCE	SOURCE	IDENTIFIER
Antibodies		
rabbit anti-GFP primary antibody	ThermoFisher	#A6455
donkey Anti-Rabbit Dylight® 488	ThermoFisher	#SA5-10038
Chemicals, Peptides, and Recombinant Proteins		
Dimethyl Hydantoin Formaldehyde	Entomopraxis	N/A
Paraformaldehyde	Sigma-Aldrich	#158127-5G
Dapi	Sigma-Aldrich	#D9542-1MG
Vectashield® H-1000	Vector Laboratories	#H-1000
reduced glutation	Sigma-Aldrich	#G-4251
Abdominal-B-HD protein	This paper	N/A
Critical Commercial Assays		
Qiagen DNeasy Blood & Tissue extraction kit	Qiagen	#69506
Nucleospin Gel and PCR Clean-Up Kit	Machery-Nagel	#740609
E.Z.N.A.® Plasmid Mini Kit I	Omega Bio-tek	#D6942-01
Quick-DNA™ Miniprep Plus Kit	Zymo Research	#D4069
LightShift™ Chemiluminiscent EMSA Kit	ThermoFisher Scientific	#20148
TurboBlotter Kit	GE Healthcare Life Sciences	#10416314
Deposited Data		
Raw and analyzed data	This paper	Mendeley: http://dx.doi.org/10.17632/xjvz2m8z6r.1 (DOI: 10.17632/xjvz2m8z6r.1)
Genitalia Bristle Number	This paper	Figshare: https://doi.org/10.6084/m9.figshare.6972707.v1
Alignment of 18C05 sequence from <i>D. santomea</i> SYN2005 and <i>D. yakuba</i> (Ivory Cost)	This paper	Figshare: https://doi.org/10.6084/m9.figshare.6972707.v1
Twelve substitutions are fixed in <i>D. santomea</i> 18C05	This paper	Figshare: https://doi.org/10.6084/m9.figshare.6972707.v1
Sex comb tooth number in <i>D. yakuba</i> and <i>D. santomea</i> and <i>D. melanogaster scute</i> mutants	This paper	Figshare: https://doi.org/10.6084/m9.figshare.6972707.v1
Hypandrial bristle number in pure species and F1 hybrids	This paper	Figshare: https://doi.org/10.6084/m9.figshare.6972740.v3
Test of various <i>UAS</i> -reporter constructs with <i>DC-GAL4</i>	This paper	Figshare: https://doi.org/10.6084/m9.figshare.6972740.v3

<i>Achaete-scute GAL4</i> lines and their hypandrial bristle phenotype with <i>Dcr2</i> ; <i>UAS-singed.RNAi</i> ¹⁰⁵⁷⁴	This paper	Figshare: https://doi.org/10.6084/m9.figshare.6972740.v3
Cloning strategy	This paper	Figshare: https://doi.org/10.6084/m9.figshare.6972740.v3
18C05_D. san_A1200.4	This paper	GenBank #MG460738
18C05_D. san_car1490.3	This paper	GenBank #MG460742
18C05_D. san_BS14.1	This paper	GenBank #MG460740
18C05_D. san_51.7.3_1560	This paper	GenBank #MG460737
18C05_D. san_OBAT_1200.13	This paper	GenBank #MG460744
18C05_D. san_Quija650.37	This paper	GenBank #MG460747
18C05_D. san_Quija650.22	This paper	GenBank #MG460746
18C05_D. san_Quija650.14	This paper	GenBank #MG460745
18C05_D. san_C1350.14	This paper	GenBank #MG460741
18C05_D. san_B1300.13	This paper	GenBank #MG460739
18C05_D. san_Rain42	This paper	GenBank #MG460748
18C05_D. san_Field3.4	This paper	GenBank #MG460743
18C05_D. san_STO4	This paper	GenBank #MG460749
18C05_D. san_SYN2005	This paper	GenBank #MG460750
18C05_D. yak_15.6.8	This paper	GenBank #MG460759
18C05_D. yak_LP1	This paper	GenBank #MG460761
18C05_D. yak_2.22.1	This paper	GenBank #MG460756
18C05_D. yak_4.23.1	This paper	GenBank #MG460757
18C05_D. yak_4.32.1	This paper	GenBank #MG460758
18C05_D. yak_Tai18E2	This paper	GenBank #MG460765
18C05_D. yak_Ivory Coast	This paper	GenBank #MG460760
18C05_D. yak_Tai18E2 (NCBI)	This paper	GenBank #MG460765
18C05_D. yak_PB 3.1.3	This paper	GenBank #MG460763
18C05_D. yak_PB 3.4.1	This paper	GenBank #MG460764
18C05_D. yak_PB1.4.21	This paper	GenBank #MG460762
18C05_D. yak_5.3.1	This paper	GenBank #MG460755

18C05_D. teis_(Mt. Selinda)	This paper	GenBank #MG460753
18C05_D. teis_(SDSC#14021-0257.01)	This paper	GenBank #MG460754
18C05_D. mel_BL2057	This paper	GenBank #MG460736
18C05_D. sim_w501	This paper	GenBank #MG460752
18C05_D. sim_M252	This paper	GenBank #MG460751
Experimental Models: Organisms/Strains		
<i>D.melanogaster</i> 3870	Tony Long UC Irvine, RVC 3. Collected from Riverside, California, USA in 1963	N/A
<i>D.melanogaster</i> 3844	Tony Long UC Irvine, BS1. Collected from Barcelona, Spain in 1954	San Diego Stock Center #14021-0231.60
<i>D.melanogaster</i> 3841	Tony Long UC Irvine, BOG1. Collected from Bogota, Colombia in 1962	San Diego Stock Center #14021-0231.59
<i>D.melanogaster</i> 3852	Tony Long UC Irvine, KSA2. Collected in 1963	San Diego Stock Center #14021-0231.64
<i>D.melanogaster</i> 3864	Tony Long UC Irvine, KI2. Collected from Israel in 1954	San Diego Stock Center # 14021-0231.68
<i>D.melanogaster</i> T.7	Tony Long UC Irvine, Collected from Taiwan in 1968	San Diego Stock Center #14021-0231.07
<i>D.melanogaster</i> T.4	Tony Long UC Irvine, Collected from Kuala Lumpur, Malaysia in 1962	San Diego Stock Center #14021-0231.04
<i>D.melanogaster</i> 3875	Tony Long UC Irvine, VAG1. Collected from Athens, Greece in 1965	San Diego Stock Center #14021-0231.69
<i>D.melanogaster</i> 3886	Tony Long UC Irvine, Wild 5B. Collected from Red Top Mountain, Georgia in 1966	N/A
<i>D.melanogaster</i> T.1	Tony Long UC Irvine, Collected from Ica, Peru in 1956	San Diego Stock Center #14021-0231.04
<i>D.melanogaster</i> 3839	Tony Long UC Irvine, BER1. Collected from Bermudas in 1954.	San Diego Stock Center # 14021-0231.58
<i>D.melanogaster</i> 3846	Tony Long UC Irvine, CA1. Collected from Cape Town, South Africa.	San Diego Stock Center #14021-0231.62

<i>D.melanogaster</i> Sam	Tony Long UC Irvine, DSPR line. originally from TFC Mackay Sam; ry506	N/A
<i>D.melanogaster</i> iso-1 y[1]; Gr22b[iso-1] Gr22d[iso-1] cn[1] CG33964[iso-1] bw[1] sp[1]; LysC[iso-1] MstProx[iso-1] GstD5[iso-1] Rh6[1]	Bloomington Stock Center	Bloomington Stock Center #2057
<i>D.melanogaster</i> Canton-S	Roger Karess	Kyoto DGGR #105666
<i>D.melanogaster</i> dor[4]/C(1)RM, y[1] w[1] f[1]	Bloomington Stock Center	Bloomington Stock Center #35
<i>D.melanogaster</i> Nup98-96[339]/TM3, Sb[1]	Bloomington Stock Center	Bloomington Stock Center #4951
<i>D.melanogaster</i> Df(3R)D605/TM3, Sb[1] Ser[1]	Bloomington Stock Center	Bloomington Stock Center #823
<i>D.melanogaster</i> DC002 w1118; Dp(1;3)DC002, PBac{DC002}VK00033	Bloomington Stock Center	Bloomington Stock Center #30213
<i>D.melanogaster</i> DC003 w1118; Dp(1;3)DC003, PBac{DC003}VK00033	Bloomington Stock Center	Bloomington Stock Center #30214
<i>D.melanogaster</i> DC004 w1118; Dp(1;3)DC004, PBac{DC004}VK00033/TM6C, Sb1	Bloomington Stock Center	Bloomington Stock Center #30215
<i>D.melanogaster</i> DC006 w1118; Dp(1;3)DC006, PBac{DC006}VK00033/TM6C, Sb1	Bloomington Stock Center	Bloomington Stock Center #30217
<i>D.melanogaster</i> DC097 w1118; Dp(1;3)DC097, PBac{DC097}VK00033/TM6C, Sb1	Bloomington Stock Center	Bloomington Stock Center #31440
<i>D.melanogaster</i> DC098 w1118; Dp(1;3)DC098, PBac{DC098}VK00033	Bloomington Stock Center	Bloomington Stock Center #31441
<i>D.melanogaster</i> DC007 w1118; Dp(1;3)DC007, PBac{DC007}VK00033/TM6C, Sb1	Bloomington Stock Center	Bloomington Stock Center #30218
<i>D.melanogaster</i> DC008 w1118; Dp(1;3)DC008, PBac{DC008}VK00033	Bloomington Stock Center	Bloomington Stock Center #30745
<i>D.melanogaster</i> DC009 w1118; Dp(1;3)DC009, PBac{DC009}VK00033	Bloomington Stock Center	Bloomington Stock Center #30219
<i>D.melanogaster</i> DC012 w1118; Dp(1;3)DC012, PBac{DC012}VK00033	Bloomington Stock Center	Bloomington Stock Center #30222
<i>D.melanogaster</i> DC099 w1118; Dp(1;3)DC099, PBac{DC099}VK00033	Bloomington Stock Center	Bloomington Stock Center #30749
<i>D.melanogaster</i> DC013 w1118; Dp(1;3)DC013, PBac{DC013}VK00033	Bloomington Stock Center	Bloomington Stock Center #30746
<i>D.melanogaster</i> DC014 w1118; Dp(1;3)DC014, PBac{DC014}VK00033	Bloomington Stock Center	Bloomington Stock Center #31434
<i>D.melanogaster</i> DC400 w1118; Dp(1;3)DC400, PBac{DC400}VK00033	Bloomington Stock Center	Bloomington Stock Center #30795
<i>D.melanogaster</i> DC019 w1118; Dp(1;3)DC019, PBac{DC019}VK00033	Bloomington Stock Center	Bloomington Stock Center #30223
<i>D.melanogaster</i> DC436 w1118; Dp(1;3)DC436, PBac{DC436}VK00033/TM6C, Sb1	Bloomington Stock Center	Bloomington Stock Center #33487
<i>D.melanogaster</i> DC401 w1118; Dp(1;3)DC401, PBac{DC401}VK00033	Bloomington Stock Center	Bloomington Stock Center #30796
<i>D.melanogaster</i> DC-GAL4 yw ; DC-GAL4 , UAS-GFP /TM6B UAS-forked.RNAi ³³²⁰⁰	V. Stamatakis (Pat Simpson lab) Vienna Stock Center	N/A VDRC #33200

<i>D.melanogaster</i> UAS-singed.RNAi ¹⁰⁵⁷⁴⁷	Vienna Stock Center	VDRC #105747
<i>D.melanogaster</i> UAS-forked.RNAi ²⁴⁶³²	Vienna Stock Center	VDRC #24632
<i>D.melanogaster</i> UAS-ac.RNAi ¹⁰⁰⁶⁴⁷	Vienna Stock Center	VDRC #100647
<i>D.melanogaster</i> UAS-singed.RNAi ³²⁵⁷⁹	Vienna Stock Center	VDRC #32579
<i>D.melanogaster</i> UAS-forked.RNAi ¹⁰³⁸¹³	Vienna Stock Center	VDRC #103813
<i>D.melanogaster</i> UAS-sc.RNAi ¹⁰⁵⁹⁵¹	Vienna Stock Center	VDRC #105951
<i>D.melanogaster</i> yw; UAS-y y[1] w[1118]; P{w[+mC]=UAS-y.C}MC1	Vienna Stock Center	Bloomington Stock Center #3043
<i>D.melanogaster</i> yw;UAS-y TM3/pnr-GAL4	Mark Rebeiz.	N/A
<i>D.melanogaster</i> UAS-mCD8-GFP GFP transgene on second chromosome	Veronique Brodu	N/A
<i>D.melanogaster</i> w,UAS-Dcr2 ; Pin/CyO	Bloomington Stock Center	Bloomington Stock Center #24644
<i>D.melanogaster</i> UAS-scute	Bloomington Stock Center	Bloomington Stock Center #51672
<i>D.melanogaster</i> GFP-sc GFP inserted at the <i>scute</i> locus by CRISPR-mediated homologous recombination, which produces Scute protein with GFP sequence fused at the N terminus.	F. Schweisguth, [65]	N/A
<i>D.melanogaster</i> yw;UAS-Abd-B.RNAi ⁵¹¹⁶⁷	Bloomington Stock Center	Bloomington Stock Center #51167
<i>D.melanogaster</i> yw; UAS-Abd-B.RNAi ²⁶⁷⁴⁶	Bloomington Stock Center	Bloomington Stock Center #26746
<i>D.melanogaster</i> yw; NP5130-GAL4	Kyoto DGGR	Kyoto DGGR #109126
<i>D.melanogaster</i> yw; NP6333-GAL4	Kyoto DGGR	Kyoto DGGR #113920
<i>D. simulans</i>	Collected by J. R. David from Marrakech, Morocco in 2010	N/A
<i>D. mauritiana</i>	Collected by J. R. David from Mauritius Island in 1985	N/A
<i>D. sechellia</i> GFP w[1] ; pBac(3xP3-EGFPafm)::MCS:::(pW8 mini-white)	San Diego Species Stock Center	San Diego Stock Center #14021-0248.32
<i>D. yakuba</i> Ivory Coast	D. L. Stern, Collected from Ivory Coast in 1955	San Diego Stock Center #14021-0261.00
<i>D. yakuba</i> 15.6.8, Isofemale stock	Collected by D. R. Matute in São Tomé at altitude 110m in 2009	N/A
<i>D. yakuba</i> yellow[1]	San Diego Species Stock Center	San Diego Species Stock Center #14021-0261.05
<i>D. yakuba</i> 4.23.1, Isofemale stock	Collected by D. R. Matute in São Tomé at altitude 1070m in 2009	N/A
<i>D. yakuba</i> LP1, Isofemale stock	Collected by D. R. Matute in São Tomé at altitude 0m in 2009	N/A
<i>D. yakuba</i> 2.22.1, Isofemale stock	Collected by D. R. Matute	Given by D. Matute. Isofemale stock, collected in São Tomé at altitude 1250m in 2009 by D. Matute

<i>D. yakuba</i> PB1.4.21, Isofemale stock	Collected by D. R. Matute	Given by D. Matute. Isofemale stock, collected in Bioko at altitude 1300m in 2009 by D. Matute
<i>D. santomea</i> SYN2005, Mix of six isofemale lines	Given by D. Matute. collected by J. Coyne at the field station Bom Sucesso (elevation 1,150 m) in 2005	N/A
<i>D. santomea</i> STO.4	D. L. Stern, Collected in São Tomé in 1998	San Diego Stock Center #14021-0271.00
<i>D. santomea</i> Quija 650.22, Isofemale stock	Collected by D. R. Matute in São Tomé at altitude 650m in 2009	N/A
<i>D. santomea</i> Quija 650.37, Isofemale stock	Given by D. R. Matute, collected in São Tomé at altitude 650m in 2005 by Lucio Primo Monteiro under the supervision of Daniel Lachaise.	N/A
<i>D. santomea</i> Quija 650.14, Isofemale stock	Given by D. R. Matute, collected in São Tomé at altitude 650m in 2005 by Lucio Primo Monteiro under the supervision of Daniel Lachaise	N/A
<i>D. santomea</i> BS14.1, Isofemale stock	Collected by D. R. Matute in São Tomé at altitude 1150m in 2009	N/A
<i>D. santomea</i> CAR1490.3, Isofemale stock	Collected by D. R. Matute collected in São Tomé at altitude 1490m in 2009	N/A
<i>D. santomea</i> B1300.13, Isofemale stock	Collected by D. R. Matute in São Tomé at altitude 1300m in 2009	N/A
<i>D. santomea</i> OBAT1200.3, Isofemale stock	Collected by D. R. Matute collected in São Tomé at altitude 1200m in 2009	N/A
<i>D. santomea</i> A1200.4, Isofemale stock	Collected by D. R. Matute	Given by D. Matute. Isofemale stock, collected in São Tomé at altitude 1200m in 2009 by D. Matute
<i>D. santomea</i> C1350.14, Isofemale stock	Collected by D. R. Matute	Given by D. Matute. Isofemale stock, collected in São Tomé at altitude 1350m in 2009 by D. Matute

<i>D. santomea</i> Rain42, Isofemale stock	Collected by D. R. Matute	Given by D. Matute. Isofemale stock, collected in São Tomé at altitude 1240m in 2009 by D. Matute
<i>D. santomea</i> Field3.4, Isofemale stock	Collected by D. R. Matute in São Tomé at altitude 1250m in 2009	N/A
<i>D. teissieri</i>	Collected by J. R. David in Mt Selinda, Zimbabwe in 1970	N/A
<i>D. teissieri</i> #14021-0257.01	San Diego Stock Center	San Diego Stock Center # 14021-0257.01
<i>D. orena</i> , Isofemale stock	Collected by J. R. David in 1975 in Cameroon	N/A
<i>D. erecta</i>	Collected by D. Lachaise in La Lopé, Gabon in 2005	N/A
<i>D. elegans</i>	B. Prud'homme, Collected in Hong-Kong.	San Diego Stock Center # 14027-0461.03.
<i>D. melanogaster</i> <i>sc</i> ^{M6} <i>sc</i> [M6]/ <i>FM7i</i> , <i>P</i> { <i>w</i> [+ <i>mC</i>]= <i>ActGFP</i> } <i>JMR3</i>	Bloomington Stock Center	#52668
<i>D. melanogaster</i> <i>ac</i> ^{CAM1} <i>y</i> [1] <i>P</i> { <i>w</i> [+ <i>mW.hs</i>]= <i>GawB</i> } <i>CG32816</i> [<i>NP6014</i>] <i>ac</i> [<i>cam1</i>]	Bloomington Stock Center	#36540
<i>D. melanogaster</i> <i>sc</i> ⁶ <i>sc</i> [6] <i>w</i> [<i>a</i>]	Bloomington Stock Center	#108
<i>D. melanogaster</i> <i>ase</i> ¹ <i>Df</i> (1) <i>ase-1</i> , <i>sc</i> [<i>ase-1</i>] <i>pn</i> [1]/ <i>C</i> (1) <i>DX</i> , <i>y</i> [1] <i>f</i> [1]	Bloomington Stock Center	#104
<i>D. melanogaster</i> <i>sc</i> ⁵ <i>y</i> [1] <i>sc</i> [5]	Bloomington Stock Center	#178
<i>D. melanogaster</i> <i>ac</i> ¹ <i>y</i> [1] <i>ac</i> [1] <i>w</i> [1118]; <i>P</i> { <i>w</i> [+ <i>mC</i>]= <i>GAL4-ac.13</i> }1	Bloomington Stock Center	#8715
<i>D. melanogaster</i> <i>sc</i> ¹ <i>y</i> [1] <i>sc</i> [1]	Bloomington Stock Center	#176
<i>D. melanogaster</i> <i>ac</i> ^{sbm} <i>ac</i> [<i>sbm</i>]	Given by P. Simpson	N/A
<i>D. melanogaster</i> <i>ac</i> ^{Hw-1} <i>Df</i> (1) <i>sc</i> 10-1, <i>sc</i> [10-1]/ <i>y</i> [1] <i>ac</i> [<i>Hw-1</i>]	Bloomington Stock Center	#109
<i>D. melanogaster</i> <i>sc</i> ²⁹ <i>In</i> (1) <i>sc</i> [29], <i>sc</i> [29] <i>w</i> [<i>a</i>] <i>eag</i> [<i>sc</i> 29]	Bloomington Stock Center	#1442
<i>D. melanogaster</i> <i>ac</i> ¹ <i>sc</i> ¹ <i>y</i> [1] <i>ac</i> [1] <i>sc</i> [1] <i>pn</i> [1]	Bloomington Stock Center	#4596
<i>D. melanogaster</i> <i>sc</i> ^H <i>C</i> (1) <i>DX</i> , <i>y</i> [1] <i>f</i> [1]; <i>T</i> (1;4) <i>sc</i> [<i>H</i>], <i>sc</i> [<i>H</i>]	Bloomington Stock Center	#4055
<i>D. melanogaster</i> <i>sc</i> ⁹ <i>In</i> (1) <i>sc</i> [9], <i>sc</i> [9] <i>w</i> [<i>a</i>] <i>f</i> [1] <i>Bx</i> [1]	DGRC Kyoto Stock Center	#102028
<i>D. melanogaster</i> <i>sc</i> ^{S2} <i>T</i> (1;2) <i>sc</i> [<i>S2</i>], <i>y</i> [+] <i>sc</i> [<i>S2</i>]: <i>cn</i> [1] <i>M</i> (2)53[1]/+; <i>CyO</i>	Bloomington Stock Center	#3333
<i>D. melanogaster</i> <i>sc</i> ⁷ <i>Df</i> (1) <i>B</i> / <i>In</i> (1) <i>sc</i> [7], <i>In</i> (1) <i>AM</i> , <i>sc</i> [7] <i>ptg</i> [4]	Bloomington Stock Center	#723
<i>D. melanogaster</i> <i>ac</i> ³ <i>sc</i> ¹⁰⁻¹ <i>In</i> (1) <i>ac</i> [3], <i>sc</i> [10-1] <i>ac</i> [3] <i>w</i> [1] <i>sable</i> [1]/ <i>FM7i</i> , <i>P</i> { <i>w</i> [+ <i>mC</i>]= <i>ActGFP</i> } <i>JMR3</i>	Bloomington Stock Center	#36541
<i>D. melanogaster</i> <i>sc</i> ⁴ <i>In</i> (1) <i>sc</i> [4], <i>y</i> [1] <i>sc</i> [4] <i>ABO-X</i> [1]	Bloomington Stock Center	#789

<i>D. melanogaster</i> sc ⁸ <i>T(1;3)sc[260-15], sc[260-15]/FM6 B[1] dm[1] sc[8] y[31d]</i>	Bloomington Stock Center	#842
<i>D. melanogaster</i> ac ¹ sc ¹⁹ <i>Df(1)sc[19]/y[1] ac[1]; Dp(1;2)sc[19]/In(2L)Cy, S[2] Cy[1]</i>	Bloomington Stock Center	#3822
<i>D. melanogaster</i> VT054793-GAL4	Vienna Drosophila Research Center	VT054793
<i>D. melanogaster</i> VT054794-GAL4	Vienna Drosophila Research Center	VT054794
<i>D. melanogaster</i> VT054795-GAL4	Vienna Drosophila Research Center	VT054795
<i>D. melanogaster</i> VT054796-GAL4	Vienna Drosophila Research Center	VT054796
<i>D. melanogaster</i> VT054798-GAL4	Vienna Drosophila Research Center	VT054798
<i>D. melanogaster</i> VT054799-GAL4	Vienna Drosophila Research Center	VT054799
<i>D. melanogaster</i> GMR14C10-GAL4	Janelia Research Campus	GMR14C10
<i>D. melanogaster</i> GMR15B10-GAL4	Janelia Research Campus	GMR15B10
<i>D. melanogaster</i> GMR15C11-GAL4	Janelia Research Campus	GMR15C11
<i>D. melanogaster</i> GMR15X09-GAL4	This paper	N/A
<i>D. melanogaster</i> VT054805-GAL4	Vienna Drosophila Research Center	VT054805
<i>D. melanogaster</i> GMR15A01-GAL4	Janelia Research Campus	GMR15A01
<i>D. melanogaster</i> GMR14C12-GAL4	Janelia Research Campus	GMR14C12
<i>D. melanogaster</i> GMR15A04-GAL4	Janelia Research Campus	GMR15A04
<i>D. melanogaster</i> GMR15C10-GAL4	Janelia Research Campus	GMR15C10
<i>D. melanogaster</i> GMR15E07-GAL4	Janelia Research Campus	GMR15E07
<i>D. melanogaster</i> GMR15E09-GAL4	Janelia Research Campus	GMR15E09
<i>D. melanogaster</i> GMR13D04-GAL4	Janelia Research Campus	GMR13D04
<i>D. melanogaster</i> GMR13C08-GAL4	Janelia Research Campus	GMR13C08
<i>D. melanogaster</i> GMR12H02-GAL4	Janelia Research Campus	GMR12H02
<i>D. melanogaster</i> GMR13B12-GAL4	Janelia Research Campus	GMR13B12
<i>D. melanogaster</i> VT054820-GAL4	Vienna Drosophila Research Center	VT054820
<i>D. melanogaster</i> VT054821-GAL4	Vienna Drosophila Research Center	VT054821
<i>D. melanogaster</i> VT054822b-GAL4	This paper	N/A
<i>D. melanogaster</i> VT054823-GAL4	Vienna Drosophila Research Center	VT054823
<i>D. melanogaster</i> VT054824-GAL4	Vienna Drosophila Research Center	VT054824
<i>D. melanogaster</i> VT054825-GAL4	Vienna Drosophila Research Center	VT054825
<i>D. melanogaster</i> VT054826-GAL4	Vienna Drosophila Research Center	VT054826

<i>D. melanogaster</i> VT054827-GAL4	Vienna Drosophila Research Center	VT054827
<i>D. melanogaster</i> VT054828-GAL4	Vienna Drosophila Research Center	VT054828
<i>D. melanogaster</i> VT054829-GAL4	Vienna Drosophila Research Center	VT054829
<i>D. melanogaster</i> VT054831-GAL4	Vienna Drosophila Research Center	VT054831
<i>D. melanogaster</i> VT054832-GAL4	Vienna Drosophila Research Center	VT054832
<i>D. melanogaster</i> GMR18G09-GAL4	Janelia Research Campus	GMR18G09
<i>D. melanogaster</i> VT054833-GAL4	Vienna Drosophila Research Center	VT054833
<i>D. melanogaster</i> GMR18E07-GAL4	Janelia Research Campus	GMR18E07
<i>D. melanogaster</i> VT054834-GAL4	Vienna Drosophila Research Center	VT054834
<i>D. melanogaster</i> GMR19D04-GAL4	Janelia Research Campus	GMR19D04
<i>D. melanogaster</i> VT054835-GAL4	Vienna Drosophila Research Center	VT054835
<i>D. melanogaster</i> VT054836-GAL4	Vienna Drosophila Research Center	VT054836
<i>D. melanogaster</i> GMR18C05-GAL4	Janelia Research Campus	GMR18C05
<i>D. melanogaster</i> GMR19B11-GAL4	Janelia Research Campus	GMR19B11
<i>D. melanogaster</i> VT054838-GAL4	Vienna Drosophila Research Center	VT054838
<i>D. melanogaster</i> GMR18G07-GAL4	Janelia Research Campus	GMR18G07
<i>D. melanogaster</i> VT054839-GAL4	Vienna Drosophila Research Center	VT054839
<i>D. melanogaster</i> GMR18F05-GAL4	Janelia Research Campus	GMR18F05
<i>D. melanogaster</i> VT054840-GAL4	Vienna Drosophila Research Center	VT054840
<i>D. melanogaster</i> VT054841-GAL4	Vienna Drosophila Research Center	VT054841
<i>D. melanogaster</i> GMR19A06-GAL4	Janelia Research Campus	GMR19A06
<i>D. melanogaster</i> VT054842-GAL4	Vienna Drosophila Research Center	VT054842
<i>D. melanogaster</i> GMR18E10-GAL4	Janelia Research Campus	GMR18E10
<i>D. melanogaster</i> VT054843-GAL4	Vienna Drosophila Research Center	VT054843
<i>D. melanogaster</i> GMR20B05-GAL4	Janelia Research Campus	GMR20B05
<i>D. melanogaster</i> VT054845-GAL4	Vienna Drosophila Research Center	VT054845
<i>D. melanogaster</i> VT054846-GAL4	Vienna Drosophila Research Center	VT054846
<i>D. melanogaster</i> VT054839mel-BL2057-GAL4	This paper	VT054839mel- BL2057
<i>D. melanogaster</i> VT054839yak-GAL4	This paper	N/A
<i>D. melanogaster</i> VT054839san-GAL4	This paper	N/A

<i>E. coli</i> One Shot® TOP10	Invitrogen	#C404003
<i>E. coli</i> NEB10-beta	New England Biolabs	#C3019H
<i>E. coli</i> BL21 (DE3)	Nicolas Joly	N/A
Oligonucleotides		
Primers	This paper	Figshare: https://doi.org/10.6084/m9.figshare.6972740.v3
Recombinant DNA		
pBPGUw	Addgene, [66]	#17575
pBPSUw: GAL4 cassette of pBPGUw replaced by <i>scute</i> CDS.	This paper	N/A
15X09-pBPGUw	This paper	N/A
VT054822b-pBPGUw	This paper	N/A
VT054839yak-pBPGUw	This paper	N/A
VT054839san-pBPGUw	This paper	N/A
18C05_T7-pBPGUw	This paper	N/A
18C05_BL2057-pBPGUw	This paper	N/A
18C05Yakfull-pBPGUw	This paper	N/A
18C05Sanfull-pBPGUw	This paper	N/A
18C05AmelBL-pBPGUw	This paper	N/A
18C05BmelBL-pBPGUw	This paper	N/A
18C05CmelBL-pBPGUw	This paper	N/A
18C05ABmelBL-pBPGUw	This paper	N/A
18C05BCmelBL-pBPGUw	This paper	N/A
18C05Asan-pBPGUw	This paper	N/A
18C05Bsan-pBPGUw	This paper	N/A
18C05Ayak-pBPGUw	This paper	N/A
18C05Byak-pBPGUw	This paper	N/A
18C05Cyak-pBPGUw	This paper	N/A
VT054839mel-BL2057-pBPGUw	This paper	N/A
VT054839yak-pBPGUw	This paper	N/A
VT054839san-pBPGUw	This paper	N/A
18C05_SSSY-pBPSUw	This paper	N/A
18C05_YYSS-pBPSUw	This paper	N/A
18C05_SSYS-pBPSUw	This paper	N/A
18C05_SYYY-pBPSUw	This paper	N/A
18C05_YYYS-pBPSUw	This paper	N/A
18C05_SSYy-pBPSUw	This paper	N/A
18C05_YYSY-pBPSUw	This paper	N/A
18C05_YSYY-pBPSUw	This paper	N/A
18C05_YSSY-pBPSUw	This paper	N/A
18C05yakT970A-pBPSUw	This paper	N/A
18C05YakT1429G-pBPSUw	This paper	N/A
18C05yakA1507G-pBPSUw	This paper	N/A
18C05yakt1775G-pBPSUw	This paper	N/A
18C05_Anc-pBPSUw	This paper	N/A
18C05_AncT1008C-pBPSUw	This paper, GeneScript	N/A
18C05_AncT1429G-pBPSUw	This paper, GeneScript	N/A
18C05_AncT1482C-pBPSUw	This paper, GeneScript	N/A
18C05_AncA1507G-pBPSUw	This paper, GeneScript	N/A
18C05_AncT1775G-pBPSUw	This paper, GeneScript	N/A
18C05_yakG869A-pBPSUw	This paper, GeneScript	N/A
18C05_yakT1008C-pBPSUw	This paper, GeneScript	N/A

18C05_yakT1482C-pBPSUw	This paper, GeneScript	N/A
18C05_AncG869A-pBPSUw	This paper, GeneScript	N/A
18C05_AncT670G-pBPSUw	This paper, GeneScript	N/A
18C05_Anc-SNPall-pBPSUw	This paper, GeneScript	N/A
Abd-B-HD-pGEX-4T-1	S. B. Carroll, [46]	N/A
Software and Algorithms		
Nebuilder Tools	New England Biolabs	https://nebuilder.neb.com/
Jaspar	[43]	http://jaspar.genereg.net
R 3.4	[60]	https://cran.r-project.org/
ImageJ	[37]	https://imagej.nih.gov/ij/download.html
Geneious	Biomatters Ltd.	https://www.geneious.com/download/

824